

# A MESHLESS LOCAL GALERKIN METHOD FOR THE NUMERICAL SOLUTION OF HAMMERSTEIN INTEGRAL EQUATIONS BASED ON THE MOVING LEAST SQUARES TECHNIQUE

Pouria Assari

**Abstract** In this paper, a computational scheme is proposed to estimate the solution of one- and two-dimensional Fredholm-Hammerstein integral equations of the second kind. The method approximates the solution using the discrete Galerkin method based on the moving least squares (MLS) approach as a locally weighted least squares polynomial fitting. The discrete Galerkin technique for integral equations results from the numerical integration of all integrals in the system corresponding to the Galerkin method. Since the proposed method is constructed on a set of scattered points, it does not require any background meshes and so we can call it as the meshless local discrete Galerkin method. The implication of the scheme for solving two-dimensional integral equations is independent of the geometry of the domain. The new method is simple, efficient and more flexible for most classes of nonlinear integral equations. The error analysis of the method is provided. The convergence accuracy of the new technique is tested over several Hammerstein integral equations and obtained results confirm the theoretical error estimates.

**Keywords** Hammerstein integral equation, discrete Galerkin method, moving least squares (MLS), meshless method, error analysis.

**MSC(2010)** 65D10, 45G99, 65G99.

## 1. Introduction

Many problems of mathematical physics, engineering and mechanics can be stated in the form of nonlinear integral equations [25, 44, 51]. These types of integral equations also arise as a reformulation of boundary value problems with a certain nonlinear boundary condition. Consider nonlinear  $d$ -dimensional Fredholm-Hammerstein integral equations of the second kind as follows:

$$u(\mathbf{x}) - \lambda \int_D K(\mathbf{x}, \mathbf{y}) \Phi(\mathbf{y}, u(\mathbf{y})) d\mathbf{y} = f(\mathbf{x}), \quad \mathbf{x}, \mathbf{y} \in D \subset \mathbb{R}^d, \quad (1.1)$$

where the kernel function  $K(\mathbf{x}, \mathbf{y})$  and the right-hand side function  $f(\mathbf{x})$  are given, the unknown function  $u(\mathbf{x})$  must be determined,  $\lambda$  is a non-zero constant,  $D$  is a

---

Email address: [passari@basu.ac.ir](mailto:passari@basu.ac.ir)  
Department of Mathematics, Faculty of Sciences, Bu-Ali Sina University,  
Hamedan 65178, Iran

$d$ -dimensional closed domain and the known function  $\Phi$  is continuous and nonlinear respect to the variable  $u$ .

Several methods have been proposed for the numerical solution of Hammerstein integral equations. The discrete collocation-type method [37, 38], the discrete collocation method [16], Walsh-Hybrid functions [46], the collocation method and positive definite functions [3], the discrete Legendre spectral method [22] the modified iterated projection method [29], the Adomian decomposition method [51] and wavelet methods [2, 34] have been investigated to solve one-dimensional Hammerstein integral equations. The iterated discrete Galerkin method [31], the iterated collocation method [28, 32], the Galerkin method with spline functions as basis [20], the Nystrom method [13, 30], two-dimensional rationalized Haar (RH) functions [17], the two-dimensional differential transform (TDDT) method [50], the degenerate method (DM) [1], fast collocation methods [21], piecewise polynomial projection methods [48], the Nystrom method [13, 30] and the Gauss product quadrature rules [18] have been applied to solve two-dimensional Hammerstein integral equations of the second kind.

The MLS scheme as a general case of Shepard's method has been introduced by Lancaster and Salkauskas [39]. The MLS consists of a local weighted least squares fitting, valid on a small neighborhood of a point and only based on the information provided by its closet points. This approach is recognized as a meshless method because it is based on a set of scattered points and consequently does not need any domain elements. The MLS methodology is an effective and simple technique for approximating unknown functions. A valuable advantage of using the MLS is that it sets up and solves many small systems, instead of a single, but large system [26, 52]. The MLS has significant importance applications in different problems of computational mathematics such as partial differential equations and a large number of papers have presented many numerical methods for solving them.

We would like to review some of the most recent works for the numerical solution of integral equations utilizing the meshless methods. The meshless discrete collocation schemes have been investigated using radial basis functions (RBFs) for solving linear and nonlinear integral equations on non-rectangular domains with sufficiently smooth kernels [6, 7] and weakly singular kernels [12]. The RBFs have been applied for the numerical solution of the one-dimensional linear Fredholm and Volterra integral equations [27] and Volterra-Fredholm-Hammerstein integral equations [47]. The meshless product integration (MPI) method [10] has been proposed to solve one-dimensional linear weakly singular integral equations. The MLS collocation method has been used for solving linear and nonlinear two-dimensional integral equations on non-rectangular domains [9, 45] and integro-differential equations [23]. Authors of [41] have introduced a meshless Galerkin method for solving boundary integral equations. An MLS-based meshless method [8] has been utilized to solve weakly singular linear integral equations of the second kind.

This article presents a numerical method based on the MLS method for solving one- and two-dimensional Fredholm-Hammerstein integral equations of the second kind. The scheme is based on the discrete Galerkin method with the shape functions of the MLS approximation constructed on scattered points as a basis. To apply Galerkin methods for two-dimensional integral equations on non-rectangular regions, we must divide the solution region into non-overlapping triangular fragments [14, 33]. Therefore by using the MLS scheme as a meshless approach, we can solve two-dimensional integral equations without any mesh generation on the

domain. The numerical approach developed on the current paper utilizes the Gauss-Legendre quadrature rule for approximating integrals. The presented scheme does not depend on the geometry of the domain and does not increase the difficulties for higher dimensional problems due to the easy adaption of MLS. The implementation of the scheme on computers is simple and also obtains accurate results. Moreover, the approach can be expanded to other classes of integral equations. The error analysis of the new method is provided. Some numerical examples are given to illustrate the efficiency and accuracy of the technique.

The outline of the current paper is as follows: In Section 2, we represent some basic formulations and properties of the MLS approximation. In Section 3, a numerical method is investigated to solve the Hammerstein integral equation (1.1) by combining the MLS approximation and the discrete Galerkin method. In Section 4, the error bound and the convergence rate of the presented method are obtained. Numerical examples are considered in Section 5. Finally, the article is concluded in Section 6.

## 2. The MLS approximation

Given data values of the function  $u(\mathbf{x})$  at certain data sites  $X = \{\mathbf{x}_1, \dots, \mathbf{x}_N\}$  in the closed domain  $D \subset \mathbb{R}^d$ . The idea of the MLS method is to approximate  $u(\mathbf{x})$  for every point  $\mathbf{x} \in D$  in a weighted least squares sense. For  $\mathbf{x} \in D$ , the value  $s_{u,X}(\mathbf{x})$  of the MLS approximation is given by the solution of

$$\min \left\{ \sum_{i=1}^N [u(\mathbf{x}_i) - p(\mathbf{x}_i)]^2 w(\mathbf{x}, \mathbf{x}_i) : p \in \Pi_q(\mathbb{R}^d) \right\}, \quad (2.1)$$

where  $w : D \times D \rightarrow [0, +\infty)$  is a continuous weight function and  $\Pi_q(\mathbb{R}^d)$  is the linear space of polynomials of total degree less than or equal to  $q$  in  $d$  variables with the basis  $\{p_1, \dots, p_Q\}$  [52]. We are mainly interested in local continuous weight function  $w$  which gets smaller as its arguments move away from each other. Ideally,  $w$  vanishes for arguments  $\mathbf{x}, \mathbf{y} \in D$  when  $\|\mathbf{x} - \mathbf{y}\|_2$  is greater than a certain threshold. Therefore, we can assume that

$$w(\mathbf{x}, \mathbf{y}) = \Gamma_\delta(\mathbf{x} - \mathbf{y}) = \gamma \left( \frac{\|\mathbf{x} - \mathbf{y}\|_2}{\delta} \right), \quad \delta > 0,$$

where  $\Gamma$  is a radial function, meaning that  $\Gamma(\mathbf{x}) = \gamma(\|\mathbf{x}\|_2)$ ,  $\mathbf{x} \in \mathbb{R}^d$ , in which  $\gamma$  is a univariate and nonnegative function,  $\gamma : [0, \infty) \rightarrow \mathbb{R}$ , with the property  $\gamma(r) = 0$  when  $r \geq 1$  [52].

In the following theorem, we will find a direct approach to obtain the solution of the problem (2.1), but prior to that we present the following definition.

**Definition 2.1** ([19, 52]). We call a set of points  $X = \{\mathbf{x}_1, \dots, \mathbf{x}_N\} \subset \mathbb{R}^d$  as  $q$ -unisolvent if the only polynomial of total degree at most  $q$ , interpolating zero data on  $X$  is the zero polynomial.

**Theorem 2.1** ([52]). Suppose that for every  $\mathbf{x} \in D$  the set  $\{\mathbf{x}_1, \dots, \mathbf{x}_N\}$  is  $q$ -unisolvent. In this situation, the problem (2.1) is uniquely solvable and the solution

$s_{u,X}(\mathbf{x})$  can be represented as

$$s_{u,X}(\mathbf{x}) = \sum_{i=1}^N \psi_i(\mathbf{x})u(\mathbf{x}_i), \quad (2.2)$$

where the basis functions  $\psi_i(\mathbf{x})$  are determined by

$$\psi_i(\mathbf{x}) = w(\mathbf{x}, \mathbf{x}_i) \sum_{k=1}^Q z_k p_k(\mathbf{x}_i), \quad (2.3)$$

in which the coefficients  $z_1, \dots, z_Q$  are a unique solution of

$$\sum_{k=1}^Q z_k \sum_{i=1}^N w(\mathbf{x}, \mathbf{x}_i) p_k(\mathbf{x}_i) p_l(\mathbf{x}_i) = p_l(\mathbf{x}), \quad 1 \leq l \leq Q.$$

**Remark 2.1.** It should be noted that the moving least squares approximation based on a vector of the  $d$ -variable complete monomial basis polynomials has the inherent instability. The shifted and scaled polynomial basis function can be used to improve stability of the MLS approximation [40]. In practical computations, the argument  $\mathbf{x}$  in  $\mathbf{p}(\mathbf{x})$  is usually replaced by  $\frac{\mathbf{x}-\mathbf{x}^e}{\sigma}$  to shift the origin to a fixed point  $\mathbf{x}^e = [x_1^e, \dots, x_d^e]^t$  on  $\mathfrak{R}(\mathbf{x})$  with scale factor  $\sigma > 0$ , where  $\mathfrak{R}(\mathbf{x})$  denotes the influence domain of  $\mathbf{x}$  [42].

To obtain a general algorithm of the MLS approximation, we formulate the expansion (2.2) with the matrix form

$$s_{u,X}(\mathbf{x}) = U^t \Psi(\mathbf{x}),$$

where

$$\Psi(\mathbf{x}) = [\psi_1(\mathbf{x}), \dots, \psi_N(\mathbf{x})]^t, \quad U = [u(\mathbf{x}_1), \dots, u(\mathbf{x}_N)]^t.$$

Now, to determine  $\Psi(\mathbf{x})$ , we define the matrices  $\mathbf{P}$  and  $\mathbf{W}(\mathbf{x})$  as

$$\mathbf{P}^t = [\mathbf{p}^t(\mathbf{x}_1), \mathbf{p}^t(\mathbf{x}_2), \dots, \mathbf{p}^t(\mathbf{x}_N)]_{Q \times N}, \quad \mathbf{W}(\mathbf{x}) = \begin{bmatrix} w(\mathbf{x}, \mathbf{x}_1) \cdots & 0 \\ \cdots & \ddots & \cdots \\ 0 & \cdots & w(\mathbf{x}, \mathbf{x}_N) \end{bmatrix}_{N \times N}.$$

As a conclusion from Theorem 2.1, we have

$$\Psi^t(\mathbf{x}) = \mathbf{p}^t(\mathbf{x}) A^{-1}(\mathbf{x}) B(\mathbf{x}),$$

or

$$\psi_j(\mathbf{x}) = \sum_{k=1}^Q \mathbf{p}_k(\mathbf{x}) [A^{-1}(\mathbf{x}) B(\mathbf{x})]_{kj},$$

where the matrices  $A(\mathbf{x})$  and  $B(\mathbf{x})$  are defined by

$$A(\mathbf{x}) = \mathbf{P}^t \mathbf{W} \mathbf{P} = B(\mathbf{x}) \mathbf{P} = \sum_{j=1}^N w(\mathbf{x}, \mathbf{x}_j) \mathbf{p}(\mathbf{x}_j) \mathbf{p}^t(\mathbf{x}_j),$$

and

$$B(\mathbf{x}) = \mathbf{P}^t \mathbf{W} = [w(\mathbf{x}, \mathbf{x}_1)\mathbf{p}(\mathbf{x}_1), w(\mathbf{x}, \mathbf{x}_2)\mathbf{p}(\mathbf{x}_2), \dots, w(\mathbf{x}, \mathbf{x}_N)\mathbf{p}(\mathbf{x}_N)].$$

The Gaussian and spline weight functions are applied in the present work, respectively as

$$w(\mathbf{x}, \mathbf{x}_j) = \begin{cases} \frac{\exp[-(d_j/\alpha)^2] - \exp[-(\delta/\alpha)^2]}{1 - \exp[-(\delta/\alpha)^2]}, & 0 \leq d_j \leq \delta, \\ 0, & d_j > \delta, \end{cases}$$

and

$$w(\mathbf{x}, \mathbf{x}_j) = \begin{cases} 1 - 6(d_j/\delta)^2 + 8(d_j/\delta)^3 - 3(d_j/\delta)^4, & 0 \leq d_j \leq \delta, \\ 0, & d_j > \delta, \end{cases}$$

where  $d_j = \|\mathbf{x} - \mathbf{x}_j\|_2$  (the Euclidean distance between  $\mathbf{x}$  and  $\mathbf{x}_j$ ),  $\delta$  is the size of the support domain and  $\alpha$  is a constant controlling the shape of the weight function  $w(\mathbf{x}, \mathbf{x}_j)$  which determines the weights allocated to any points in the support domain. In fact, if we chose a small value for  $\alpha$  then the effect of the point  $\mathbf{x}_j$  increases in comparison with other points.

In the following, the error analysis of the MLS method is studied which follows mostly from [26, 52]. Here, we restrict ourselves to domains satisfying an interior cone condition defined as follows [52]:

**Definition 2.2** ([52]). A set  $D \subset \mathbb{R}^d$  is said to satisfy an interior cone condition if there exists an angle  $\theta \in (0, \pi/2)$  and a radius  $r > 0$  such that for every  $\mathbf{x} \in D$  a unit vector  $\xi(\mathbf{x})$  exists such that the cone

$$C(\mathbf{x}, \xi(\mathbf{x}), \theta, r) = \{\mathbf{x} + \lambda \mathbf{y} : \mathbf{y} \in \mathbb{R}^d, \|\mathbf{y}\|_2 = 1, \mathbf{y}^T \xi(\mathbf{x}) \geq \cos \theta, \lambda \in [0, r]\},$$

is contained in  $D$ .

Now, we give some definitions from [26, 52] that are important to measure the quality of data points and to estimate the rates of convergence in the MLS method and other meshless methods.

**Definition 2.3** ([26]). The fill distance of a set of points  $X = \{\mathbf{x}_1, \dots, \mathbf{x}_N\} \subseteq D$  for a bounded domain  $D$  is defined by

$$h_{X,D} = \sup_{\mathbf{x} \in D} \min_{0 \leq j \leq N} \|\mathbf{x} - \mathbf{x}_j\|_2.$$

**Definition 2.4** ([26]). The separation distance of  $X = \{\mathbf{x}_1, \dots, \mathbf{x}_N\}$  is defined by

$$q_X = \frac{1}{2} \min_{i \neq j} \|\mathbf{x}_i - \mathbf{x}_j\|_2.$$

The set  $X$  is said to be quasi-uniform with respect to a constant  $c > 0$  if

$$q_X \leq h_{X,D} \leq cq_X.$$

In the following, we can represent a theorem from [26, 52] about the error bound for approximating a function using the MLS approximation, for every sample point  $\mathbf{x} \in D$ .

**Theorem 2.2** ([52]). *Define  $D^*$  as the closure of  $\cup_{\mathbf{x} \in D} B(\mathbf{x}, 2\tau h_0)$ . Then there exists a constant  $C > 0$  that can be computed explicitly such that for all  $u \in C^{q+1}(D^*)$  and all quasi-uniform  $X \subset D$  with  $h_{X,D} \leq h_0$ , the approximation error is bounded as follows*

$$\|u - s_{u,X}\|_\infty \leq Ch_{X,D}^{q+1} |u|_{C^{q+1}(D^*)}. \quad (2.4)$$

The semi-norm on the right-hand side is defined by

$$|u|_{C^{q+1}(D^*)} = \max_{|\alpha|=q+1} \|D^\alpha u\|_{L^\infty(D^*)}.$$

Note that, Armentano and Duran [5] proved error estimates in  $L^\infty$ , for the function and its derivatives in the one-dimensional case. The error estimates in  $L^\infty$  and  $L^2$  norms for one and higher dimensions are investigated in [4]. Also, Xiaolin Li [40] obtained the error estimates for the MLS approximation in the  $H^k$  norm in two dimensions when nodes and weight functions satisfy certain conditions. In [43], error estimation of the MLS is given in the  $W^{k,q}$  norm in  $n$  dimensions under weaker regularity assumption that  $u$  belongs to  $W^{p+1,q}$ . This weaker regularity assumption can reduce the requirement of  $u$  in Theorem 2.2 for the error estimation of the MLS method.

### 3. Solving integral equations

In this section, we present a numerical method to solve Fredholm-Hammerstein integral equations of the second kind (1.1). Let the nonlinear function  $\Phi$  in the integral equation (1.1) satisfy the following assumptions [35, 37]:

(1) There exists  $C_1 > 0$  such that

$$|\Phi(\mathbf{x}, u_1) - \Phi(\mathbf{x}, u_2)| \leq C_1 |u_1 - u_2|, \quad \text{for all } u_1, u_2 \in \mathbb{R}.$$

(2) There is a constant  $C_2 > 0$  such that  $\frac{\partial \Phi}{\partial u}$  confirms

$$\left| \frac{\partial \Phi}{\partial u}(\mathbf{x}, u_1) - \frac{\partial \Phi}{\partial u}(\mathbf{x}, u_2) \right| \leq C_1 |u_1 - u_2|, \quad \text{for all } u_1, u_2 \in \mathbb{R}.$$

(3)  $\Phi(\cdot, u(\cdot)), \frac{\partial \Phi}{\partial u}(\cdot, u(\cdot)) \in C(D)$  for  $u(x) \in C(D)$ .

**Remark 3.1.** It should be noted that if  $\Phi$  is smooth on  $D \times \mathbb{R}$  (that is, it is several times continuously differentiable) then it satisfies the conditions (1)–(3).

Suppose  $X = \{\mathbf{x}_1, \dots, \mathbf{x}_N\}$  is  $N$  nodal points randomly selected on the domain  $D$ . We estimate the unknown function  $u(\mathbf{x})$  by the MLS approximation as

$$u(\mathbf{x}) \approx \bar{u}_N(\mathbf{x}) = \sum_{j=1}^N \bar{c}_j \psi_j(\mathbf{x}), \quad \mathbf{x} \in D, \quad (3.1)$$

where  $\{\psi_1(\mathbf{x}), \dots, \psi_N(\mathbf{x})\}$  are the shape functions of the MLS method corresponding to the set  $X$ , and the coefficients  $\{\bar{c}_1, \dots, \bar{c}_N\}$  are found by solving the next system.

Assume  $V$  is the framework of some complete function space on  $D$ , such as  $L^2(D)$ , with respect to the inner product

$$\langle f, g \rangle = \int_D f(\mathbf{x})g(\mathbf{x})d\mathbf{x}, \quad f, g \in V.$$

By replacing the expansion (3.1) in the integral equation (1.1) instead of  $u(\mathbf{x})$  and taking inner product  $\langle \cdot, \psi_i \rangle$  upon both sides, we obtain

$$\begin{aligned} & \sum_{j=1}^N \bar{c}_j \int_D \psi_j(\mathbf{x}) \psi_i(\mathbf{x}) d\mathbf{x} - \lambda \int_D \int_D K(\mathbf{x}, \mathbf{y}) \Phi \left( \mathbf{y}, \sum_{j=1}^N \bar{c}_j \psi_j(\mathbf{y}) \right) \psi_i(\mathbf{x}) d\mathbf{y} d\mathbf{x} \\ &= \int_D \psi_i(\mathbf{x}) f(\mathbf{x}) d\mathbf{x}. \end{aligned}$$

Thus the method reduces the solution of the Hammerstein integral equation to the solution of a nonlinear system of algebraic equations. The iteration methods, for example Newton's method, for solving such cumbersome nonlinear system is usually sensitive to the selection of initial guess [37]. As a remedy, we recommend the following new approach based on the use of the method in [37].

Define

$$z(\mathbf{x}) = \Psi(\mathbf{x}, u(\mathbf{x})).$$

Solve the equivalent equation

$$z(\mathbf{x}) = \Psi \left( \mathbf{x}, f(\mathbf{x}) + \lambda \int_D K(\mathbf{x}, \mathbf{y}) z(\mathbf{y}) d\mathbf{y} \right), \quad \mathbf{x} \in D, \quad (3.2)$$

and obtain  $u(\mathbf{x})$  from

$$u(\mathbf{x}) = f(\mathbf{x}) + \lambda \int_D K(\mathbf{x}, \mathbf{y}) z(\mathbf{y}) d\mathbf{y}. \quad (3.3)$$

Similarly, we estimate the unknown function  $z(\mathbf{x})$  by selecting  $N$  nodal points such as  $X = \{\mathbf{x}_1, \dots, \mathbf{x}_N\}$  using the MLS approximation as follows:

$$z(\mathbf{x}) \approx \bar{z}_N(\mathbf{x}) = \sum_{j=1}^N \bar{z}_j \psi_j(\mathbf{x}), \quad \mathbf{x} \in D. \quad (3.4)$$

We replace the expansion (3.4) with  $z(\mathbf{x})$  and take the inner product  $\langle \cdot, \psi_i \rangle$  upon both sides. Thus the following nonlinear system is obtained

$$\sum_{j=1}^N \bar{z}_j \int_D \psi_j(\mathbf{x}) \psi_i(\mathbf{x}) d\mathbf{x} = \int_D \Phi \left( \mathbf{x}, f(\mathbf{x}) + \lambda \sum_{j=1}^N \bar{z}_j \int_D K(\mathbf{x}, \mathbf{y}) \psi_j(\mathbf{y}) d\mathbf{y} \right) \psi_i(\mathbf{x}) d\mathbf{x}. \quad (3.5)$$

The discrete Galerkin methods result from the numerical integration of all integrals in the system (3.5) associated with the Galerkin method. The integrals on the right-side of (3.5) need to be evaluated only once, since they are dependent only on the basis, not on the unknowns. Let the functions  $K$  and  $\Phi$  be smooth on  $D \times D$  and  $D \times (-\infty, +\infty)$ , respectively, i.e., they are several times continuously differentiable. Based upon the dimension of the integral equation (1.1), we choose quadrature formulae to approximate the integrals in the system (3.5).

### 3.1. One-dimensional integral equations

In this situation, we assume  $D = [a, b]$ . To estimate the integrals in the nonlinear system (3.5), we utilize the composite  $m_N$ -point Gauss-Legendre rule with  $M$  uniform subdivisions relative to the coefficients  $\{v_k\}$  and weights  $\{w_k\}$  in the interval

$[-1, 1]$ . Suppose  $P_{m_N}(x)$  is the well-known Legendre polynomial of order  $m_N$  with roots  $v_k$ ,  $k = 1, \dots, m_N$ , and  $g \in C^{2m_N}[-1, 1]$  then [49]

$$\int_a^b g(x)dx = \frac{\Delta x}{2} \sum_{k=1}^{m_N} w_k \sum_{q=1}^M g(\theta_k^q) + \mathcal{O}\left(\frac{1}{M^{2m_N}}\right), \quad (3.6)$$

where

$$\Delta x = \frac{b-a}{M}, \quad w_k = \frac{2}{(k+1)P'_{m_N+1}(v_k)P_{m_N}(v_k)}, \quad \text{and } \theta_k^q = \frac{\Delta x}{2}v_k + \left(q - \frac{1}{2}\right)\Delta x.$$

Since the Gaussian and spline weight functions used in the current paper are several times continuously differentiable, i.e.,  $\psi_j, \psi_i \in C^{2m_N}[a, b]$  for every  $m_N \in \mathbb{N}$ . Therefore, by applying the quadrature rule (3.6) for the integrals emerged from the left-hand side of (3.5), we obtain

$$\int_a^b \psi_j(x)\psi_i(x)dx \approx \frac{\Delta x}{2} \sum_{k=1}^{m_N} w_k \sum_{q=1}^M \psi_j(\theta_k^q)\psi_i(\theta_k^q). \quad (3.7)$$

At first, to approximate the integrals on the right side of (3.5), we apply the quadrature rule (3.6) for computing the internal integrals as follows:

$$\int_a^b K(x, y)\psi_j(y)dy \approx \frac{\Delta y}{2} \sum_{r=1}^{m_N} w_r \sum_{p=1}^M K(x, \eta_r^p)\psi_j(\eta_r^p), \quad (3.8)$$

where  $\Delta y = \frac{b-a}{M}$  and  $\eta_r^p = \frac{\Delta y}{2}v_r + \left(p - \frac{1}{2}\right)\Delta y$ . Again using the quadrature rule (3.6) for external integrals, we obtain

$$\begin{aligned} \int_a^b \Phi \left( x, f(x) + \lambda \sum_{j=1}^N \bar{z}_j \int_a^b K(x, y)\psi_j(y)dy \right) \psi_i(x)dx &\approx \frac{\Delta x}{2} \sum_{k=1}^{m_N} w_r \\ &\times \sum_{q=1}^M \Phi \left( \theta_r^p, f(\theta_r^p) + \lambda \sum_{j=1}^N \bar{z}_j \frac{\Delta y}{2} \sum_{r=1}^{m_N} w_k \sum_{p=1}^M K(\theta_r^p, \eta_k^q)\psi_j(\eta_k^q) \right) \psi_i(\theta_r^p), \end{aligned} \quad (3.9)$$

where  $\Delta x = \frac{b-a}{M}$  and  $\theta_r^p = \frac{\Delta x}{2}v_r + \left(p - \frac{1}{2}\right)\Delta x$ .

Utilizing the numerical integration schemes (3.7) and (3.9) in the system (3.5) yields the nonlinear system of algebraic equations

$$\begin{aligned} \sum_{j=1}^N \hat{z}_j \frac{\Delta x}{2} \sum_{k=1}^{m_N} w_k \sum_{q=1}^M K(x, \theta_k^q)\psi_j(\theta_k^q) &= \frac{\Delta x}{2} \sum_{r=1}^{m_N} w_r \\ &\times \sum_{p=1}^M \Phi \left( \eta_r^p, f(\eta_r^p) + \lambda \sum_{j=1}^N \hat{z}_j \frac{\Delta x}{2} \sum_{k=1}^{m_N} w_k \sum_{q=1}^M K(\eta_r^p, \theta_k^q)\psi_j(\theta_k^q) \right) \psi_i(\eta_r^p), \end{aligned}$$

for the unknowns  $\hat{Z} = [\hat{z}_1, \dots, \hat{z}_N]$ . The solution of this system eventually leads to the following numerical solution which can be approximated  $z(x)$  as:

$$\hat{z}_N(x) = \sum_{j=1}^N \hat{z}_j \psi_j(x), \quad a \leq x \leq b.$$



Finally, we find the numerical solution of the integral equation (1.1) by

$$\hat{u}_N(x) = f(x) + \lambda \frac{\Delta x}{2} \sum_{k=1}^{m_N} w_k \sum_{q=1}^M K(x, \theta_k^q) \hat{z}_N(\theta_k^q).$$

### 3.2. Two-dimensional integral equations

Suppose that  $D \subseteq [a, b] \times [a, b]$  is a two-dimensional normal domain with a smooth boundary, so we can assume that

$$D = \{(x_1, x_2) \in \mathbb{R}^2 : a \leq x_1 \leq b \text{ and } \alpha_1(x_1) \leq x_2 \leq \alpha_2(x_1)\},$$

where  $a, b \in \mathbb{R}$  and  $\alpha_1(x_1), \alpha_2(x_1) \in C^{2m_N}[a, b]$ .

For approximating the integrals in the nonlinear system (3.5), we expand the Gauss-Legendre rule to two-dimensional normal domains. If  $f(x_1, x_2) \in C^{2m_N}(D)$ , then the reduction formula for the double integrals gives

$$\int_D f(x_1, x_2) dx_1 dx_2 = \int_a^b \int_{\alpha_1(x_1)}^{\alpha_2(x_1)} f(x_1, x_2) dx_1 dx_2 = \int_0^1 F(x_1) dx_1.$$

The integral  $\int_a^b F(x_1) dx_1$  can be approximated by a composite  $m_N$ -point Gauss-Legendre quadrature rule using  $M$  subintervals relative to the coefficients  $\{\nu_k\}$  and weights  $\{w_k\}$  in the interval  $[-1, 1]$ . Thus, in the  $x_1$  direction, we can write

$$\int_a^b F(x_1) dx_1 = \frac{\Delta x_1}{2} \sum_{q=1}^M \sum_{k=1}^{m_N} w_k F(\theta_k^q) + \mathcal{O}\left(\frac{1}{M^{2m_N}}\right),$$

where  $\Delta x_1 = \frac{b-a}{M}$  and  $\theta_k^q = \frac{\Delta x_1}{2} \nu_k + (q - \frac{1}{2}) \Delta x_1$ . For each node  $\theta_k^q$ , the approximate evaluation of the integral  $F(\theta_k^q)$  is carried out by a composite  $m_N$ -point Gauss-Legendre quadrature rule using  $M$  subintervals relative to the coefficients  $\{\tau_p\}$  and weights  $\{w_p\}$  in the interval  $[-1, 1]$

$$F(\theta_k^q) = \int_{\alpha_1(\theta_k^q)}^{\alpha_2(\theta_k^q)} f(\theta_k^q, x_2) dx_2 = \frac{\Delta s(\theta_k^q)}{2} \sum_{r=1}^M \sum_{p=1}^{m_N} w_p f(\theta_k^q, \eta_p^r) + \mathcal{O}\left(\frac{1}{M^{2m_N}}\right),$$

where  $\Delta x_2(\theta_k^q) = \frac{\alpha_2(\theta_k^q) - \alpha_1(\theta_k^q)}{M}$  and  $\eta_p^r = \frac{\Delta x_2}{2} \tau_p + (r - \frac{1}{2}) \Delta x_2$ .

By choosing a suitable weight function, we find that  $\psi_j, \psi_i \in C^{2m_N}(D)$  are several times continuously differentiable. Therefore, we obtain

$$\int_D \psi_j(x_1, x_2) \psi_i(x_1, x_2) dx_1 dx_2 \approx \frac{b-a}{2M} \sum_{q=1}^M \sum_{k=1}^{m_N} w_k I[i, j, k, q], \quad (3.10)$$

where

$$I[i, j, k, q] = \frac{\Delta x_2(\theta_k^q)}{2} \sum_{r=1}^M \sum_{p=1}^{m_N} w_p \psi_j(\theta_k^q, \eta_p^r) \psi_i(\theta_k^q, \eta_p^r).$$

Similarly, based on the use of this quadrature rule, we estimate the internal integrals on the right side of (3.5) as

$$\int_D K(x_1, x_2, y_1, y_2) \psi_j(y_1, y_2) dy_1 dy_2 \approx \frac{b-a}{2M} \sum_{q'=1}^M \sum_{k'=1}^{m_N} w'_k H_1[j, k', q'](x_1, x_2), \quad (3.11)$$

where

$$H_1[j, k', q'](x_1, x_2) = \frac{\Delta s(\theta_{k'}^{q'})}{2} \sum_{r'=1}^M \sum_{p'=1}^{m_N} w_{p'} K(x_1, x_2, \theta_{k'}^{q'}, \eta_{p'}^{r'}) \psi_j(\theta_{k'}^{q'}, \eta_{p'}^{r'}).$$

Therefore, replacing the quadrature (3.11) and replicating this scheme for external integrals, we conclude that

$$\begin{aligned} \int_D \Phi \left( x_1, x_2, f(x_1, x_2) + \lambda \sum_{j=1}^N \bar{z}_j \int_D K(x_1, x_2, y_1, y_2) \psi_j(y_1, y_2) dy_1 dy_2 \right) \\ \times \psi_i(x_1, x_2) dx_1 dx_2 \approx \frac{b-a}{2M} \sum_{q=1}^M \sum_{k=1}^{m_N} w_k H_2[j, k, q, k', q'](\bar{z}_1, \dots, \bar{z}_N), \end{aligned} \quad (3.12)$$

where

$$\begin{aligned} H_2[j, k, q, k', q'](\bar{z}_1, \dots, \bar{z}_N) = \frac{\Delta x_2(\theta_k^q)}{2} \sum_{r=1}^M \sum_{p=1}^{m_N} w_p \Phi \left( \eta_r^p, \eta_r^p, f(\eta_r^p, \eta_r^p) \right. \\ \left. + \lambda \sum_{j=1}^N \bar{z}_j \frac{b-a}{2M} \sum_{q'=1}^M \sum_{k'=1}^{m_N} w_{k'} H_1[j, k', q'](\eta_r^p, \eta_r^p) \right) \psi_i(\eta_r^p, \eta_r^p), \end{aligned}$$

in which  $\Delta y_1 = \frac{b-a}{M}$ ,  $\theta_{k'}^{q'} = \frac{\Delta y_1}{2} \nu_k + (q - \frac{1}{2}) \Delta y_1$ ,  $\Delta y_2(\theta_{k'}^{q'}) = \frac{\alpha_2(\theta_{k'}^{q'}) - \alpha_1(\theta_{k'}^{q'})}{M}$  and  $\eta_{p'}^{r'} = \frac{\Delta y_2}{2} \tau_p + (r - \frac{1}{2}) \Delta y_2$ .

To approximate the integrals in the system (3.5) via the numerical integration rules (3.10) and (3.12), we obtain the following system of algebraic equations

$$\sum_{j=1}^N \hat{z}_j \frac{b-a}{2M} \sum_{q=1}^M \sum_{k=1}^{m_N} w_k I[i, j, k, q] = \frac{b-a}{2M} \sum_{q=1}^M \sum_{k=1}^{m_N} w_k H_2[j, k, q, k', q'](\hat{z}_1, \dots, \hat{z}_N),$$

where

$$I[i, j, k, q] = \frac{\Delta x_2(\theta_k^q)}{2} \sum_{r=1}^M \sum_{p=1}^{m_N} w_p \psi_j(\theta_k^q, \eta_p^r) \psi_i(\theta_k^q, \eta_p^r),$$

and

$$\begin{aligned} H_2[j, k, q, k', q'](\hat{z}_1, \dots, \hat{z}_N) = \frac{\Delta x_2(\theta_k^q)}{2} \sum_{r=1}^M \sum_{p=1}^{m_N} w_p \\ \times \Phi \left( \eta_r^p, \eta_r^p, f(\eta_r^p, \eta_r^p) + \lambda \sum_{j=1}^N \hat{z}_j \frac{b-a}{2M} \sum_{q'=1}^M \sum_{k'=1}^{m_N} w_{k'} H_1[j, k', q'](\eta_r^p, \eta_r^p) \right) \psi_i(\eta_r^p, \eta_r^p). \end{aligned}$$

Thus the solution of Eq. (3.2) is

$$\hat{z}_N(x_1, x_2) = \sum_{j=1}^N \hat{z}_j \Phi_j(x_1, x_2).$$

Now, we can compute the solution of the integral equation (1.1) by

$$\hat{u}_N(x_1, x_2) = f(x_1, x_2) + \frac{\lambda}{2M} \sum_{q=1}^M \sum_{k=1}^{m_N} w_k \frac{\Delta y_2(\theta_k^q)}{2} \sum_{r=1}^M \sum_{p=1}^{m_N} w_p K(x_1, x_2, \theta_k^q, \eta_p^r) \hat{z}_N(\theta_k^q, \eta_p^r).$$

Suppose  $D \subseteq [a, b] \times [a, b]$  is a normal domain with a piecewise smooth boundary, that's mean

$$D = \bar{D}_1 \cup \bar{D}_2 \cup \dots \cup \bar{D}_L,$$

where  $D_\ell$ 's are domains of the form

$$D_\ell = \{(x_1, x_2) \in \mathbb{R}^2 : a_\ell \leq x_1 \leq b_\ell \text{ and } \alpha_{\ell,1}(x_1) \leq x_2 \leq \alpha_{\ell,2}(x_1)\}, \quad \ell = 1, 2, \dots, L,$$

where  $a_\ell, b_\ell \in \mathbb{R}$  and  $\alpha_{\ell,1}(y), \alpha_{\ell,2}(y) \in C^{2m_N}[a_\ell, b_\ell]$ .

For approximating the integrals in the nonlinear system (3.5), we consider

$$\begin{aligned} \int_D \psi_j(x_1, x_1) \psi_i(x_1, x_1) dx_1 dx_2 &= \sum_{\ell=1}^L \int_{D_\ell} \psi_j(x_1, x_1) \psi_i(x_1, x_1) dx_1 dx_2 \\ &= \sum_{\ell=1}^L \int_{a_\ell}^{b_\ell} \int_{\alpha_{\ell,1}(x_1)}^{\alpha_{\ell,2}(x_1)} \psi_j(x_1, x_1) \psi_i(x_1, x_1) dx_1 dx_2. \end{aligned}$$

Therefore, by applying the integration rule (3.10), this integral can be computed as

$$\int_D \psi_j(x_1, x_1) \psi_i(x_1, x_1) dx_1 dx_2 \approx \sum_{\ell=1}^L \frac{b_\ell - a_\ell}{2M} \sum_{q=1}^M \sum_{k=1}^{m_N} w_k I_\ell[i, j, k, q],$$

where

$$I_\ell[i, j, k, q] = \frac{\Delta x_{2,\ell}(\theta_{k,\ell}^q)}{2} \sum_{r=1}^M \sum_{p=1}^{m_N} w_p \psi_j(\theta_{k,\ell}^q, \eta_{p,\ell}^r) \psi_i(\theta_{k,\ell}^q, \eta_{p,\ell}^r),$$

with

$$\begin{aligned} \Delta x_{1,\ell} &= \frac{b_\ell - a_\ell}{M}, \quad \theta_{k,\ell}^q = \frac{\Delta x_{1,\ell}}{2} \nu_k + (q - \frac{1}{2}) \Delta x_{1,\ell}, \\ \Delta x_{2,\ell}(\theta_{k,\ell}^q) &= \frac{\alpha_{2,\ell}(\theta_{k,\ell}^q) - \alpha_{1,\ell}(\theta_{k,\ell}^q)}{M} \quad \text{and} \quad \eta_{p,\ell}^r = \frac{\Delta x_{2,\ell}}{2} \tau_p + (r - \frac{1}{2}) \Delta x_{2,\ell}. \end{aligned}$$

Also for the integrals in the right-hand side of the system (3.5), we first consider

$$\begin{aligned} \int_D K(x_1, x_2, y_1, y_2) \psi_j(y_1, y_2) dy_1 dy_2 &= \sum_{\ell=1}^L \int_{a_\ell}^{b_\ell} \int_{\alpha_{\ell,1}(x_1)}^{\alpha_{\ell,2}(x_1)} K(x_1, x_2, y_1, y_2) \\ &\quad \times \psi_j(y_1, y_2) dy_1 dy_2 \approx \frac{b - a}{2M} \sum_{q'=1}^M \sum_{k'=1}^{m_N} w_{k'} H_{1,\ell}[j, k', q'](x_1, x_2), \end{aligned}$$

where

$$H_{1,\ell}[j, k', q'](x_1, x_2) = \frac{\Delta y_2(\theta_{k',\ell}^{q'})}{2} \sum_{r'=1}^M \sum_{p'=1}^{m_N} w_{p'} K(x_1, x_2, \theta_{k',\ell}^{q'}, \eta_{p',\ell}^{r'}) \psi_j(\theta_{k',\ell}^{q'}, \eta_{p',\ell}^{r'}),$$

with

$$\Delta y_{1,\ell} = \frac{b_\ell - a_\ell}{M}, \quad \theta_{k',\ell}^{q'} = \frac{\Delta y_{1,\ell}}{2} \nu_k + (q - \frac{1}{2}) \Delta y_{1,\ell},$$

$$\Delta y_{2,\ell}(\theta_{k',\ell}^{q'}) = \frac{\alpha_{2,\ell}(\theta_{k',\ell}^{q'}) - \alpha_{1,\ell}(\theta_{k',\ell}^{q'})}{M} \quad \text{and} \quad \eta_{p',\ell}^{r'} = \frac{\Delta y_{2,\ell}}{2} \tau_p + (r - \frac{1}{2}) \Delta y_{2,\ell}.$$

Next, the use of integration rule (3.12) for every  $D_\ell$  yields

$$\begin{aligned} & \int_D \Phi \left( x_1, x_2, f(x_1, x_2) + \lambda \sum_{j=1}^N \bar{z}_j \int_D K(x_1, x_2, y_1, y_2) \psi_j(y_1, y_2) dy_1 dy_2 \right) \\ & \times \psi_i(x_1, x_2) dx_1 dx_2 \approx \sum_{\ell=1}^L \frac{b_\ell - a_\ell}{2M} \sum_{q=1}^M \sum_{k=1}^{m_N} w_k H_{2,\ell}[j, k, q, k', q'](\bar{z}_1, \dots, \bar{z}_N), \end{aligned}$$

where

$$\begin{aligned} H_{2,\ell}[j, k, q, k', q'](\bar{z}_1, \dots, \bar{z}_N) &= \frac{\Delta x_{2,\ell}(\theta_{k,\ell}^q)}{2} \sum_{r=1}^M \sum_{p=1}^{m_N} w_p \Phi \left( \theta_{k,\ell}^q, \eta_{p,\ell}^r, f(\theta_{k,\ell}^q, \eta_{p,\ell}^r) \right. \\ & \left. + \lambda \sum_{j=1}^N \bar{z}_j \frac{b_\ell - a_\ell}{2M} \sum_{q'=1}^M \sum_{k'=1}^{m_N} w_{k'} H_{1,\ell}[j, k', q'](\theta_{k,\ell}^q, \eta_{p,\ell}^r) \right) \psi_i(\theta_{k,\ell}^q, \eta_{p,\ell}^r). \end{aligned}$$

Then, the nonlinear system (3.13) is converted to

$$\begin{aligned} & \sum_{j=1}^N \hat{z}_j \sum_{\ell=1}^L \frac{b_\ell - a_\ell}{2M} \sum_{q=1}^M \sum_{k=1}^{m_N} w_k I_\ell[i, j, k, q] \\ & = \sum_{\ell=1}^L \frac{b_\ell - a_\ell}{2M} \sum_{q=1}^M \sum_{k=1}^{m_N} w_k H_{2,\ell}[j, k, q, k', q'](\hat{z}_1, \dots, \hat{z}_N). \end{aligned}$$

Finally, the solution of the integral equation (1.1) is obtained by

$$\begin{aligned} \hat{u}_N(x_1, x_2) &= f(x_1, x_2) + \lambda \sum_{\ell=1}^L \frac{b_\ell - a_\ell}{2M} \sum_{q=1}^M \sum_{k=1}^{m_N} w_k \frac{\Delta y_{2,\ell}(\theta_{k,\ell}^q)}{2} \\ & \times \sum_{r=1}^M \sum_{p=1}^{m_N} w_p K(x_1, x_2, \theta_{k,\ell}^q, \eta_{p,\ell}^r) \hat{z}_N(\theta_{k,\ell}^q, \eta_{p,\ell}^r). \end{aligned}$$

**Remark 3.2.** In general form, let  $D$  be a bounded closed domain in  $\mathbb{R}^d$  and a normal domain with respect to a coordinate axis. To approximate the integral in (3.5), we require a suitable quadrature formula which depends on the classification of the domain  $D$ . We can choose a generalized composite  $m_N$ -point Gauss-Legendre numerical integration scheme over the domain  $D$  relative to the coefficients  $\{(v_{1_s}, \dots, v_{d_s})\}$  and the weights  $\{w_s\}$  with  $M$  subdivisions. Therefore, for every  $h \in C^{m_N}(D)$ , we can assume

$$\int_D h(x_1, \dots, x_d) dx_1 \dots dx_d \approx \sum_{q=1}^M \sum_{s=1}^{m_N} \bar{w}_s h(\theta_{1_s}^q(v_{1_s}, \dots, v_{d_s}), \dots, \theta_{d_s}^q(v_{1_s}, \dots, v_{d_s})).$$

Of course, the development of such integration formulae is not really easy for high dimensional integrals. Generally, the solution of the integral equation (1.1) reduces

to the solution of a linear system of algebraic equations. As can be seen, the method could be easily extended to the higher dimensional problems and it does not increase the difficulty for these problems due to the easy adaption of MLS scheme. Also the scheme is only independent of the pairwise distances between points and not the geometry of the domain and so it does not need any domain elements. It should be noted that solving high dimensional Fredholm integral equations by the proposed method can be interesting for future researches.

## 4. Error estimates

This section provides an error bound and the rate of convergence for the method proposed in this work based on those results obtained in [14, 36].

The Hammerstein operator  $\mathcal{K} : L^2(D) \rightarrow L^2(D)$  is introduced as

$$\mathcal{K}u(\mathbf{x}) = \int_D K(\mathbf{x}, \mathbf{y})\Phi(\mathbf{y}, u(\mathbf{y}))d\mathbf{y}, \quad \mathbf{x}, \mathbf{y} \in D \subset \mathbb{R}^d.$$

Therefore, we can represent the integral equation (1.1) in operator form as

$$(I - \lambda\mathcal{K})u = f.$$

We define the operator  $\mathcal{R}$  on  $L^2(D)$  as follows:

$$\mathcal{R}u(\mathbf{x}) = \Phi(\mathbf{x}, u(\mathbf{x})).$$

If we let  $z(\mathbf{x}) = \mathcal{R}u(\mathbf{x})$ , then we can solve the equivalent integral equation

$$z = \mathcal{R}(f + \lambda\mathcal{K}z),$$

for unknown  $z(\mathbf{x})$ . Then the solution of original integral equation (1.1) is obtained by

$$u(\mathbf{x}) = f + \lambda\mathcal{K}z(\mathbf{x}).$$

We define  $\mathcal{P}_N : L^2(D) \rightarrow V_N$  as a Galerkin projection operator by

$$\mathcal{P}_N z(\mathbf{x}) = \sum_{j=1}^N c_j \psi_j \mathbf{x}, \quad \mathbf{x} \in D,$$

where the space  $V_N = \text{span}\{\psi_1, \dots, \psi_N\} \subset L^2(D)$  and the coefficients  $\{c_1, \dots, c_N\}$  determined by solving the linear system

$$\langle u, \psi_j \rangle = \sum_{j=1}^N c_j \langle \psi_i, \psi_j \rangle, \quad i = 1, \dots, N,$$

where  $\langle \cdot, \cdot \rangle$  is the inner product on  $L^2(D)$ . To obtain a better understanding of  $\mathcal{P}_N$ , we give an explicit formula for  $\mathcal{P}_N z$ . We introduce a new basis  $\{\phi_1, \dots, \phi_N\}$  for  $V_N$  by using the Gram-Schmidt process to create an orthonormal basis from  $\{\psi_1, \dots, \psi_N\}$ . The element  $\phi_i$  is a linear combination of  $\{\psi_1, \dots, \psi_N\}$  and moreover

$$\langle \phi_i, \phi_j \rangle = \delta_{ij}, \quad i, j = 1, \dots, N.$$

With this new basis, it is straightforward to show that

$$\mathcal{P}_N z(\mathbf{x}) = \sum_{i=1}^N \langle z, \phi_i \rangle \phi_i(\mathbf{x}), \quad \mathbf{x} \in D.$$

Therefore the operator  $\mathcal{P}_N$  is called an orthogonal projection operator [14]. By this operator, we can represent the system (3.5) in the operator form as

$$\bar{z}_N = \mathcal{P}_N \mathcal{R}(f + \lambda \mathcal{K} \bar{z}_N).$$

Using the composite  $m_N$ -point Gauss-Legendre rule with  $M$  subdivisions over  $[-1, 1]$  relative to the coefficients  $\{v_r\}$  and weights  $\{w_k\}$ , we define a discrete semi-definite inner product for one- and two-dimensional cases respectively as follows:

$$\langle f, g \rangle \approx \langle f, g \rangle_N = \frac{1}{2M} \sum_{k=1}^{m_N} w_k \sum_{q=1}^M f(\theta_k^q) g(\theta_k^q),$$

and

$$\langle f, g \rangle \approx \langle f, g \rangle_N = \frac{1}{2M} \sum_{q=1}^M \sum_{k=1}^{m_N} w_k \frac{\Delta s(\theta_k^q)}{2} \sum_{r=1}^M \sum_{p=1}^{m_N} w_p f(\theta_k^q, \eta_p^r) g(\theta_k^q, \eta_p^r),$$

where  $\theta_k^q = \frac{1}{2M} y_k + \frac{(q-\frac{1}{2})}{M}$ ,  $\Delta s(\theta_k^q) = \frac{\alpha_2(\theta_k^q) - \alpha_1(\theta_k^q)}{M}$  and  $\eta_p^r = \frac{\Delta s}{2} s_p + (r - \frac{1}{2}) \Delta s(\theta_k^q)$ .

Now we can introduce a discrete seminorm as

$$\|g\|_N = \sqrt{\langle g, g \rangle_N}, \quad g \in L^2(D).$$

As before, we know that

$$\langle f, g \rangle = \langle f, g \rangle_N + \mathcal{O}\left(\frac{1}{M^{2m_N}}\right), \quad f, g \in L^2(D).$$

We present the discrete projection operator as

$$\mathcal{Q}_N u(\mathbf{x}) = \sum_{k=1}^N c_k \psi_k(\mathbf{x}), \quad \mathbf{x} \in D,$$

where the coefficients  $\{c_1, \dots, c_N\}$  determined by solving the linear system

$$\langle u, \psi_j \rangle_N = \sum_{k=1}^N c_k \langle \psi_k, \psi_j \rangle_N, \quad j = 1, \dots, N.$$

Now, we present the following theorem about the discrete Galerkin operator with the MLS shape functions as the basis.

**Lemma 4.1** ([9]). *Having in mind the assumptions of Theorem 2.2, suppose that  $\mathcal{Q}_N$ ,  $N \geq 1$  are the discrete orthogonal projections for the shape functions of the MLS approximation corresponding to nodal points  $X = \{(x_1, t_1), \dots, (x_N, t_N)\} \subset D \subset \mathbb{R}^d$ . Assume the family  $\{\mathcal{Q}_N : N \geq 1\}$  is uniformly bounded on  $L^2(D)$ , say  $\|\mathcal{Q}_N\| \leq m < \infty$ . If  $u \in C^{q+1}(D^*)$  then  $\mathcal{Q}_N u$  converges to  $u$  as  $N \rightarrow \infty$  and moreover*

$$\|\mathcal{Q}_N u - u\|_\infty \leq (1 + m) Ch_{X,D}^{q+1} |u|_{C^{q+1}(D^*)}. \quad (4.1)$$

**Remark 4.1.** The proof of uniformly bounded for the operators  $\{\mathcal{Q}_N\}$  has been investigated at some length in Atkinson and Bogomolny [15].

Based on the use of composite  $m_N$ -point Gauss-Legendre quadrature rule using  $M$  subintervals relative to the coefficients  $\{y_k\}$  and weights  $\{w_k\}$  in the interval  $[-1, 1]$ , a sequence of numerical integral operators  $\mathcal{K}_N$ ,  $N \geq 1$ , one- and two-dimensional cases on  $C^{2m_N}(D)$  is also introduced from the introduced quadrature rule as

$$\mathcal{K}_N u(x) = \frac{1}{2M} \sum_{k=1}^{m_N} w_k \sum_{q=1}^M w_k K(x, \theta_k^q) \Phi(\theta_k^q, u(\theta_k^q)),$$

and

$$\mathcal{K}_N u(x_1, x_2) = \frac{1}{2M} \sum_{q=1}^M \sum_{k=1}^{m_N} w_k \frac{\Delta s(\theta_k^q)}{2} \sum_{r=1}^M \sum_{p=1}^{m_N} w_p K(x_1, x_2, \theta_k^q, \eta_p^r) \Phi(\theta_k^q, \eta_p^r, u(\theta_k^q, \eta_p^r)),$$

where  $\theta_k^q = \frac{1}{2M} y_k + (q - \frac{1}{2}) \frac{1}{M}$ ,  $\Delta s(\theta_k^q) = \frac{\alpha_2(\theta_k^q) - \alpha_1(\theta_k^q)}{M}$  and  $\eta_p^r = \frac{\Delta s}{2} s_p + (r - \frac{1}{2}) \Delta s(\theta_k^q)$ .

It should be noted that  $\{\mathcal{K}_N\}$  is a collectively compact set and converges point-wise [24, 34], moreover for every  $u \in C^{(2m_N)}(D)$  and  $K \in C^{(2m_N)}(D \times D)$ , we have [24]

$$\|\mathcal{K}u - \mathcal{K}_N u\|_\infty \leq \frac{C_N}{M^{2m_N}} \sup_{x \in D} |u^{(2m_N)}(x)|. \quad (4.2)$$

We can represent the final systems in the abstract form as

$$\hat{z}_N = \mathcal{Q}_N \mathcal{R}(f + \lambda \mathcal{K}_N \hat{z}_N),$$

and so the solution of the proposed scheme in the current paper is gotten by

$$\hat{u}_N = f + \lambda \mathcal{K}_N \hat{z}_N.$$

Let  $\mathcal{F}u = u$  be a fixed point problem on  $V$  where  $V$  is the framework of some complete function space on  $D$ ,  $\mathcal{F}$  is a nonlinear compact operator on  $V$ . Define the approximating operator  $\mathcal{F}_N$  on  $V$  to estimate the operator  $\mathcal{F}$ . The required hypotheses on  $\mathcal{F}$  and  $\mathcal{F}_N$ ,  $N \geq 1$  are listed and labeled in the following [13, 16]:

**Hypothesis H1.**  $\mathcal{F}$  and  $\mathcal{F}_N$ ,  $N \geq 1$ , are completely continuous nonlinear operators on  $V$ .

**Hypothesis H2.**  $\mathcal{F}_N$ ,  $N \geq 1$  is a collectively compact family on  $V$ .

**Hypothesis H3.**  $\mathcal{F}_N$  is pointwise convergent to  $\mathcal{F}$  on  $V$ , i.e,  $\mathcal{F}_N(u) \rightarrow \mathcal{F}(u)$ ,  $u \in V$ .

**Hypothesis H4.** At each point of  $V$ ,  $\{\mathcal{F}_N\}$  is an equicontinuous family.

**Hypothesis H5.**  $\mathcal{F}$  and  $\mathcal{F}_N$ ,  $N \geq 1$  are twice Frechet differential on the ball  $B(u_0, r)$ ,  $r > 0$  and moreover

$$\|\mathcal{F}_N''\| \leq \alpha < \infty, \quad N \geq 1, \quad u \in B(u_0, r).$$

**Theorem 4.1** ([15]). *Suppose H1-H4. Let  $z_0$  be a fixed point of  $\mathcal{F}$ , and assume that 1 is not an eigenvalue of  $\mathcal{F}'(z_0)$ , where  $\mathcal{F}'(z_0)$  denotes the Frechet derivative of  $\mathcal{F}$  at  $z_0$ . If H5 is satisfied on  $B(z_0, r) \subseteq V$ , then  $u_0$  is a fixed point, of the nonzero*

index. Moreover, there are  $\varepsilon, M > 0$  such that for every  $N > M$ ,  $\mathcal{F}_N$  has a unique fixed point  $z_N$  in  $B(u_0, \varepsilon)$ . Also, there is a constant  $\gamma_1 > 0$  such that

$$\|z_N - z_0\|_\infty \leq \gamma_1 \|\mathcal{F}z_0 - \mathcal{F}_N z_0\|_\infty, \quad N \geq M. \quad (4.3)$$

This gives a bound on the rate of convergence of the iterated solution  $\bar{u}_N$  to  $u_0$ .

Consider the nonlinear operators  $\mathcal{F}z$  and  $\mathcal{F}_N z$  on  $L^2(D)$  as follows:

$$\mathcal{F}z \equiv \mathcal{R}(\mathcal{K}z + f),$$

and

$$\mathcal{F}_N z \equiv \mathcal{Q}_N \mathcal{R}(\mathcal{K}_N z + f).$$

Assuming that  $\mathcal{K}$  and  $\mathcal{K}_N$  satisfies H1-H5, it is shown in [16] that  $\mathcal{F}$  and  $\mathcal{F}_N$  also satisfies H1-H5.

We are ready to consider the convergence theorem about the presented method.

**Theorem 4.2.** *Suppose that the assumptions of Theorem 4.1 and Lemma 4.1 hold. Let the nonlinear integral equation (1.1) have a unique solution  $u_0 \in C^{q+1}(D^*) \cap C^{2m_N}(D)$ . Assume that 1 is not an eigenvalue of  $\mathcal{R}'(\mathcal{K}z_0 + f)\mathcal{K}'$ , where  $\mathcal{K}'$  and  $\mathcal{R}'$  indicates the Frechet derivatives at  $z_0 = \mathcal{R}(u_0)$ . Thus there are  $\varepsilon, \bar{M} > 0$  such that the proposed method has a unique solution  $\bar{u}_N$  in the ball  $B(u_0, \varepsilon)$  for every  $N > \bar{M}$ . Moreover there exist constants  $C, C_1, C_2, m, \gamma_1, h_0$  provided that  $h_{X,D} \leq h_0$  such that*

$$\begin{aligned} \|u_N - u_0\|_\infty \leq & |\lambda| C_2 \gamma_1 (1 + m) C h_{X,D}^{q+1} |g_0|_{C^{q+1}(D^*)} \\ & + \frac{|\lambda| (C_2 \gamma_1 m C_1 + 1) C_N}{M^{2m_N}} \sup_{x \in D} |z_0^{(2m_N)}(x)|, \end{aligned} \quad (4.4)$$

where  $g_0 \equiv \mathcal{R}(\mathcal{K}z_0 + f)$ .

**Proof.** Since 1 is not an eigenvalue of  $\mathcal{F}' \equiv \mathcal{R}'(\mathcal{K}z_0 + f)\mathcal{K}'$ , this can be immediately obtained from Theorem 4.1 that there exists a unique solution  $z_N \in B(z_0, \varepsilon)$  such that

$$\begin{aligned} \|z_N - z_0\|_\infty & \leq \gamma_1 \|\mathcal{F}z_0 - \mathcal{F}_N z_0\|_\infty = \gamma_1 \|\mathcal{R}(\mathcal{K}z_0 + f) - \mathcal{Q}_N \mathcal{R}(\mathcal{K}_N z_0 + f)\|_\infty \\ & \leq \gamma_1 \|\mathcal{R}(\mathcal{K}z_0 + f) - \mathcal{Q}_N \mathcal{R}(\mathcal{K}z_0 + f)\|_\infty + \gamma_1 \|\mathcal{Q}_N \mathcal{R}(\mathcal{K}z_0 + f) - \mathcal{Q}_N \mathcal{R}(\mathcal{K}_N z_0 + f)\|_\infty. \end{aligned}$$

Thus, there is a constant  $M_1 > 0$  such that for every  $N > M_1$ , we have  $\|z_N - z_0\|_\infty < \varepsilon$ . As before we know that the family  $\mathcal{Q}_N$ ,  $N \geq 1$  is uniformly bounded, say  $\|\mathcal{Q}_N\| \leq m < \infty$ . Therefore

$$\|z_N - z_0\|_\infty \leq \gamma_1 \|\mathcal{R}(\mathcal{K}z_0 + f) - \mathcal{Q}_N \mathcal{R}(\mathcal{K}z_0 + f)\|_\infty + \gamma_1 m \|\mathcal{R}(\mathcal{K}z_0 + f) - \mathcal{R}(\mathcal{K}_N z_0 + f)\|_\infty.$$

Based on the assumption (1), we obtain

$$\|z_N - z_0\|_\infty \leq \gamma_1 \|\mathcal{R}(\mathcal{K}z_0 + f) - \mathcal{Q}_N \mathcal{R}(\mathcal{K}z_0 + f)\|_\infty + \gamma_1 m C_1 \|\mathcal{K}z_0 - \mathcal{K}_N z_0\|_\infty.$$

In other words, by considering  $u_N = f + \lambda \mathcal{K}_N z_N$ , we have

$$\begin{aligned} \|u_N - u_0\|_\infty & \leq \|(f + \lambda \mathcal{K}_N z_N) - (f + \lambda \mathcal{K}z_0)\|_\infty = |\lambda| \|\mathcal{K}_N z_N - \mathcal{K}z_0\|_\infty \\ & \leq |\lambda| \|\mathcal{K}_N z_N - \mathcal{K}_N z_0\|_\infty + |\lambda| \|\mathcal{K}_N z_0 - \mathcal{K}z_0\|_\infty, \end{aligned} \quad (4.5)$$



so it is concluded that

$$\|u_N - u_0\|_\infty \leq |\lambda| \|\mathcal{K}_N\| \|z_N - z_0\|_\infty + |\lambda| \|\mathcal{K}_N z_0 - \mathcal{K} z_0\|_\infty. \quad (4.6)$$

Since the family  $\mathcal{K}_N$  is the pointwise convergence to  $\mathcal{K}$ , there exists a constant  $M_2 > 0$  such that for every  $N > M_2$  we have  $\|\mathcal{K}_N z_0 - \mathcal{K} z_0\|_\infty < \varepsilon$  and from the principle of uniform boundedness [14], it can be supposed that  $\|\mathcal{K}_N\| \leq C_2$ . By substituting (4.5) in (4.6), we obtain

$$\begin{aligned} \|u_N - u_0\|_\infty &\leq |\lambda| C_2 \|z_N - z_0\|_\infty + |\lambda| \|\mathcal{K}_N z_0 - \mathcal{K} z_0\|_\infty \\ &\leq |\lambda| C_2 \gamma_1 \|\mathcal{R}(\mathcal{K} z_0 + f) - \mathcal{Q}_N \mathcal{R}(\mathcal{K} z_0 + f)\|_\infty + |\lambda| (C_2 \gamma_1 m C_1 + 1) \|\mathcal{K} z_0 - \mathcal{K}_N z_0\|_\infty. \end{aligned}$$

Choosing  $\hat{M} = \max\{M_1, M_2\}$ , we deduce that  $\hat{u}_N$ , for  $N > M$ , within  $B(u_0, \hat{\varepsilon})$ , is the unique solution of the proposed method, because

$$\|u_N - u_0\|_\infty \leq |\lambda| (C_2 \varepsilon + \varepsilon) = \hat{\varepsilon}.$$

It is seen  $z_0(\mathbf{x}) = \Phi(\mathbf{x}, u_0(\mathbf{x}))$  in  $C^{q+1}(D^*) \cap C^{2m_N}(D)$ , because  $\Phi$  is a well-behaved function on  $D \times \mathbb{R}$  and  $u_0 \in C^{q+1}(D^*) \cap C^{2m_N}(D)$ . Finally using Lemma 4.1 and the error bound (4.2), we give

$$\begin{aligned} \|u_N - u_0\|_\infty &\leq |\lambda| C_2 \gamma_1 (1 + m) C h_{X,D}^{q+1} |g_0|_{C^{q+1}(D^*)} \\ &\quad + \frac{|\lambda| (C_2 \gamma_1 m C_1 + 1) C_N}{M^{2m_N}} \sup_{\mathbf{x} \in D} |z_0^{(2m_N)}(\mathbf{x})|, \end{aligned}$$

where  $g_0 \equiv \mathcal{R}(\mathcal{K} z_0 + f)$ . Since,  $h_{X,D} \rightarrow 0$  as  $N \rightarrow \infty$  (justified by the quasi-uniform condition on  $X$ ), yields  $u_N \rightarrow u_0$ . This completes the proof.  $\square$

## 5. Numerical examples

To test the efficiency and accuracy of the proposed method, four Hammerstein integral equations are solved. We utilize the Gaussian and spline weight functions via the linear ( $q = 1$ ) and quadratic ( $q = 2$ ) basis functions. We employ 10-points composite dual Gauss-Legendre quadrature rule with  $M = 10$  for approximating integrals in the scheme. Theorem 4.2 confirms that by choosing a sufficiently accurate quadrature rule, the error of the MLS approximation is dominated over the global error and so, increasing the number of the integration nodes  $m_N$  or the subintervals  $M$  has no significant effect on the error of the proposed method. In all computations, we put  $\delta = 2 \times h$  and  $\delta = 3 \times h$  for the linear and quadratic cases, respectively [45, 52]. In Gaussian weight function, we chose  $\alpha = 0.5 \times h$ . It should be noted that we have used  $h \equiv h_{X,D}$  for simplicity in notations. The results obtained in Examples 5.2 and 5.4 are compared with the method based on the use of thin plate splines of order  $k = 1, 2$  as a type of the free shape parameter radial basis functions [6, 11].

We have measured the accuracy of the presented technique by the maximum error  $\|e_N\|_\infty$  and the mean error  $\|e_N\|_2$  which can be defined for  $D \subset \mathbb{R}^d$  as follows:

$$\|e_N\|_\infty = \max_{\mathbf{x} \in D} \{|u_{ex}(\mathbf{x}) - \hat{u}_N(\mathbf{x})|\}, \quad \|e_N\|_2 = \left( \int_D |u_{ex}(\mathbf{x}) - \hat{u}_N(\mathbf{x})|^2 d\mathbf{x} \right)^{\frac{1}{2}},$$

where the exact solution  $u_{ex}(\mathbf{x})$  is estimated by the numerical solution  $\hat{u}_N(\mathbf{x})$ . The convergence rates of the presented scheme have been also reported by

$$Ratio = \frac{\ln(\|e_N\|_\infty) - \ln(\|e_{N'}\|_\infty)}{\ln(h) - \ln(h')}.$$

All calculations are run on a Laptop with 2.10 GHz of Core 2 CPU and 4 GB of RAM with the Digits environment variable assigned to be 20. To solve the final nonlinear system of algebraic equations, the FSOLVE command has been employed based on the floating-point arithmetic as an iterative process. In this command, the selection of initial guesses is important for convergence issue. Here, for  $N \leq 10$ , we choose the zero vector of length  $N$  for initial guesses [6]. To select the initial guesses for  $N > 10$ , we apply the obtained solutions corresponding to the nodal points whose number is less than  $N$ . In other words, we assume that  $\hat{u}_\tau$  is the approximate solution which is obtained by the presented method for  $\tau < N$ , then consider the following linear system of algebraic equations

$$\sum_{j=1}^N c_k^{(0)} \psi_k(\mathbf{x}_i) = \hat{u}_\tau(\mathbf{x}_i), \quad i = 1, \dots, N, \quad (5.1)$$

The initial value may be chosen as the solution of system (5.1). We can increase the value of  $\tau$  until a satisfactory convergence is achieved [6].

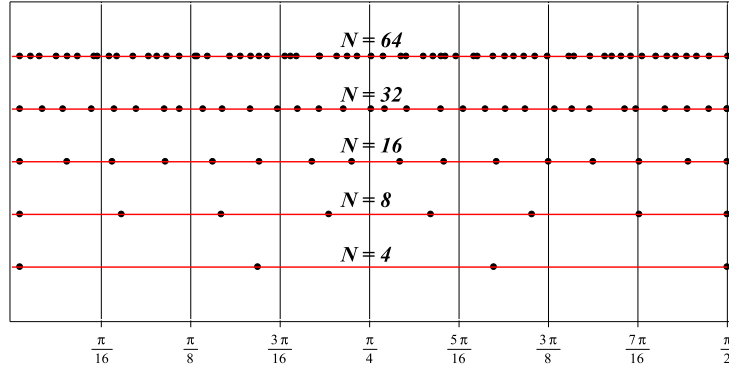


Figure 1. The consideration of nodes for Example 5.1

**Example 5.1.** Consider the following Fredholm-Hammerstein integral equation:

$$u(x) - \int_0^{\frac{\pi}{2}} \frac{\cos(x+y+\pi)}{x^2+2} \frac{e^{y^2+u(y)}}{\sqrt{y+e^2}} dy = f(x), \quad x, y \in [0, \frac{\pi}{2}], \quad (5.2)$$

where the function  $f(x)$  has been so chosen that the exact solution is

$$u_{ex}(x) = \frac{\sin(x+1)}{\sqrt{x^2+2}}.$$

The distribution of the nodes, selected randomly on the interval  $[0, \frac{\pi}{2}]$ , is depicted in Figure 1. The numerical results in terms of  $\|e_N\|_2$  and  $\|e_N\|_\infty$  at different numbers of  $N$  and the rate of convergence for the linear and quadratic basis functions

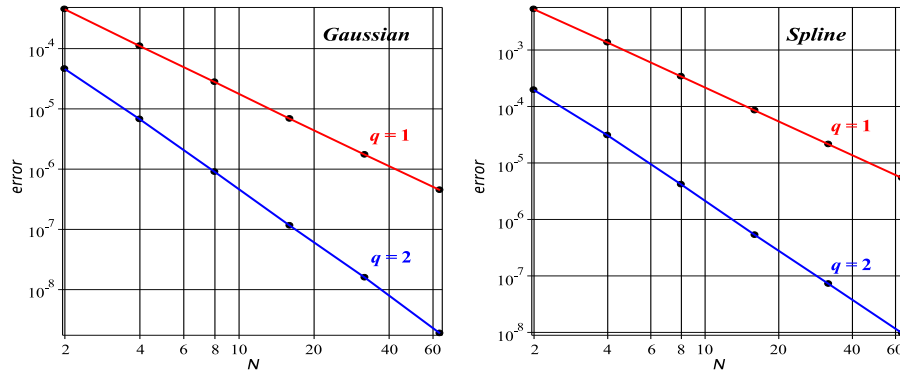


Figure 2. Absolute error distributions of Example 5.1

utilizing the Gaussian and spline weight functions are presented in Tables 1 and 2, respectively. We have compared the obtained errors for different numbers of  $N$  in the logarithmic mode in Figure 2. We see that the results gradually converge to the exact values as the number of data nodes increases and the ratio stays nearly constant ( $\approx 2$ ) for  $q = 1$  and ( $\approx 3$ ) for  $q = 2$  so, the numerical results verify the theoretical error estimates in Theorem 4.2.

Table 1. Some numerical results for Example 5.1 with Gaussian weight functions

$N$	$h$	$\ e_N\ _2$		$\ e_N\ _\infty$		Ratio	Ratio
		$q = 1$	$q = 2$	$q = 1$	$q = 2$		
2	0.250	$3.23 \times 10^{-4}$	$2.09 \times 10^{-5}$	$4.49 \times 10^{-4}$	—	$4.59 \times 10^{-5}$	—
4	0.125	$7.15 \times 10^{-5}$	$2.37 \times 10^{-6}$	$1.11 \times 10^{-4}$	2.00	$6.71 \times 10^{-6}$	2.77
8	0.062	$1.64 \times 10^{-5}$	$2.35 \times 10^{-7}$	$2.78 \times 10^{-5}$	2.01	$8.95 \times 10^{-7}$	2.90
16	0.031	$3.90 \times 10^{-6}$	$2.20 \times 10^{-8}$	$6.83 \times 10^{-6}$	2.02	$1.15 \times 10^{-7}$	2.95
32	0.015	$9.53 \times 10^{-7}$	$2.17 \times 10^{-9}$	$1.73 \times 10^{-6}$	1.97	$1.58 \times 10^{-8}$	2.86
64	0.007	$2.77 \times 10^{-7}$	$4.09 \times 10^{-10}$	$4.48 \times 10^{-7}$	1.95	$1.88 \times 10^{-9}$	3.06

Table 2. Some numerical results for Example 5.1 with spline weight functions

$N$	$h$	$\ e_N\ _2$		$\ e_N\ _\infty$		Ratio	Ratio
		$q = 1$	$q = 2$	$q = 1$	$q = 2$		
2	0.250	$2.91 \times 10^{-3}$	$9.01 \times 10^{-5}$	$5.25 \times 10^{-3}$	—	$1.95 \times 10^{-4}$	—
4	0.125	$1.01 \times 10^{-3}$	$1.47 \times 10^{-5}$	$1.35 \times 10^{-3}$	1.95	$3.07 \times 10^{-5}$	2.66
8	0.062	$2.87 \times 10^{-4}$	$1.61 \times 10^{-6}$	$3.38 \times 10^{-4}$	2.00	$4.14 \times 10^{-6}$	2.88
16	0.031	$7.58 \times 10^{-5}$	$2.71 \times 10^{-7}$	$8.46 \times 10^{-5}$	1.99	$5.28 \times 10^{-7}$	2.97
32	0.015	$1.94 \times 10^{-5}$	$1.62 \times 10^{-8}$	$2.13 \times 10^{-5}$	1.98	$7.20 \times 10^{-8}$	2.87
64	0.007	$4.91 \times 10^{-6}$	$2.40 \times 10^{-9}$	$5.38 \times 10^{-6}$	1.98	$9.61 \times 10^{-9}$	2.90

**Example 5.2.** Consider the following Fredholm-Hammerstein integral equation:

$$u(x) - \int_0^1 \frac{e^{xy+1}}{\sqrt{x+y+1}} \frac{y^2+1}{1+u^2(y)} dy = f(x), \quad x, y \in [0, 1], \quad (5.3)$$

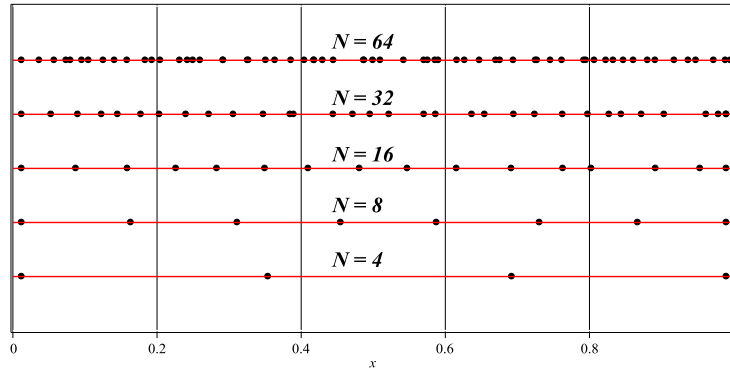


Figure 3. The consideration of nodes for Example 5.2

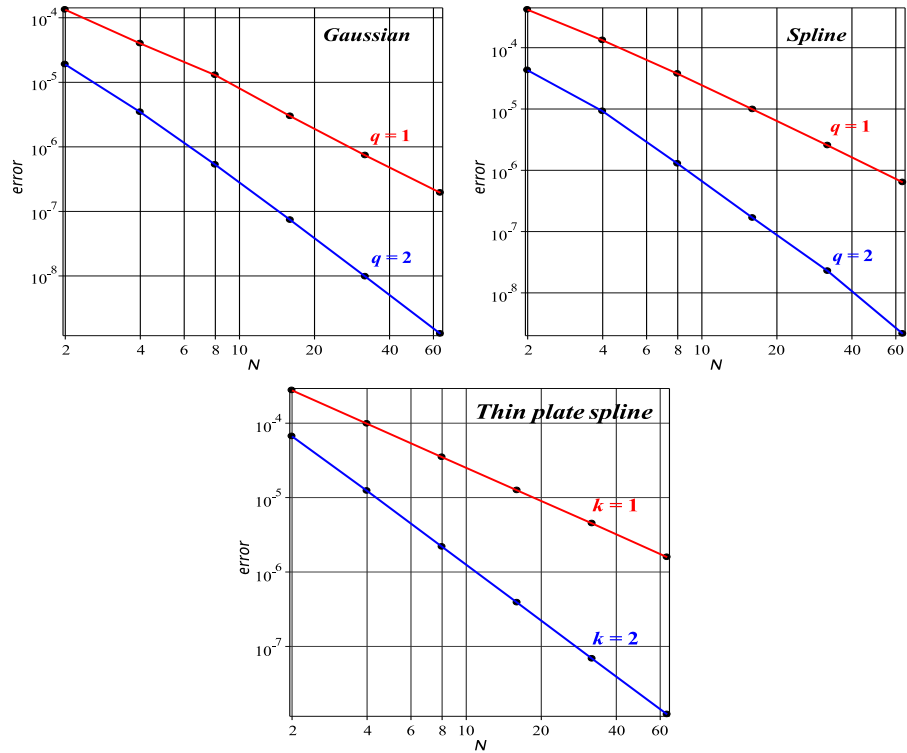


Figure 4. Absolute error distributions of Example 5.2

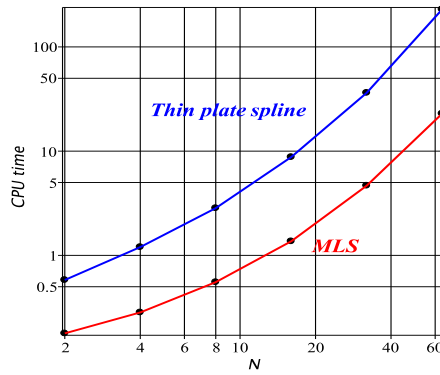


Figure 5. CPU times for Example 5.2

Table 3. Some numerical results for Example 5.2 with Gaussian weight functions

$N$	$h$	$\ e_N\ _2$		$\ e_N\ _\infty$			
		$q = 1$	$q = 2$	$q = 1$	Ratio	$q = 2$	Ratio
2	0.250	$7.85 \times 10^{-5}$	$8.59 \times 10^{-6}$	$1.33 \times 10^{-4}$	—	$1.89 \times 10^{-5}$	—
4	0.125	$1.91 \times 10^{-5}$	$1.16 \times 10^{-6}$	$3.99 \times 10^{-5}$	1.73	$3.45 \times 10^{-6}$	2.45
8	0.062	$4.30 \times 10^{-6}$	$1.29 \times 10^{-7}$	$1.29 \times 10^{-5}$	1.82	$5.28 \times 10^{-7}$	2.71
16	0.031	$9.26 \times 10^{-7}$	$1.32 \times 10^{-8}$	$2.98 \times 10^{-6}$	1.92	$7.35 \times 10^{-8}$	2.84
32	0.015	$2.02 \times 10^{-7}$	$1.31 \times 10^{-9}$	$7.63 \times 10^{-7}$	2.96	$9.76 \times 10^{-9}$	2.91
64	0.007	$4.60 \times 10^{-8}$	$1.99 \times 10^{-10}$	$1.94 \times 10^{-7}$	1.97	$1.27 \times 10^{-9}$	2.94

Table 4. Some numerical results for Example 5.2 with spline weight functions

$N$	$h$	$\ e_N\ _2$		$\ e_N\ _\infty$			
		$q = 1$	$q = 2$	$q = 1$	Ratio	$q = 2$	Ratio
2	0.250	$3.61 \times 10^{-4}$	$2.75 \times 10^{-5}$	$4.16 \times 10^{-4}$	—	$4.28 \times 10^{-5}$	—
4	0.125	$8.60 \times 10^{-5}$	$4.34 \times 10^{-6}$	$1.32 \times 10^{-4}$	1.65	$9.19 \times 10^{-6}$	2.21
8	0.062	$1.68 \times 10^{-5}$	$6.12 \times 10^{-7}$	$3.75 \times 10^{-5}$	1.81	$1.28 \times 10^{-6}$	2.83
16	0.031	$3.92 \times 10^{-6}$	$7.71 \times 10^{-8}$	$9.86 \times 10^{-6}$	1.93	$1.67 \times 10^{-7}$	2.93
32	0.015	$8.83 \times 10^{-7}$	$9.37 \times 10^{-9}$	$2.54 \times 10^{-6}$	1.95	$2.27 \times 10^{-8}$	2.88
64	0.007	$1.72 \times 10^{-7}$	$1.22 \times 10^{-9}$	$6.35 \times 10^{-7}$	1.99	$2.15 \times 10^{-9}$	2.95

Table 5. Some numerical results for Example 5.2 with thin plate splines

$N$	$h$	$\ e_N\ _2$		$\ e_N\ _\infty$			
		$k = 1$	$k = 2$	$k = 1$	Ratio	$k = 2$	Ratio
2	0.250	$1.69 \times 10^{-4}$	$3.51 \times 10^{-5}$	$2.76 \times 10^{-4}$	—	$6.65 \times 10^{-5}$	—
4	0.125	$5.84 \times 10^{-5}$	$6.42 \times 10^{-6}$	$9.83 \times 10^{-5}$	1.48	$1.23 \times 10^{-5}$	2.43
8	0.062	$2.05 \times 10^{-5}$	$1.18 \times 10^{-6}$	$3.49 \times 10^{-5}$	1.49	$2.18 \times 10^{-6}$	2.49
16	0.031	$7.35 \times 10^{-6}$	$2.12 \times 10^{-7}$	$1.25 \times 10^{-5}$	1.48	$3.88 \times 10^{-7}$	2.49
32	0.015	$2.63 \times 10^{-6}$	$3.84 \times 10^{-8}$	$4.49 \times 10^{-6}$	1.47	$6.83 \times 10^{-8}$	2.51
64	0.007	$1.03 \times 10^{-6}$	$6.89 \times 10^{-9}$	$1.58 \times 10^{-6}$	1.51	$1.22 \times 10^{-8}$	2.48

where the function  $f(x)$  has been so chosen that the exact solution is

$$u_{ex}(x) = \frac{e^{x^2-x-\pi}}{x+1}.$$

Previous numerical methods have difficulties to solve these types of integral equa-

tions, but we can easily compute the approximate solution for this problem utilizing the meshless method presented in this work based on some random nodes over the  $[0, 1]$  depicted in Figure 3. The numerical results in terms of  $\|e_N\|_2$  and  $\|e_N\|_\infty$  at different numbers of  $N$  and the rate of convergence for the linear and quadratic basis functions utilizing the Gaussian and spline weight functions are presented in Tables 3 and 4, respectively. To compare the presented method, we also solve the integral equation (5.3) utilizing the thin plate splines and the numerical results are given in Table 5. The obtained errors for different numbers of  $N$  using the presented method and the thin plate splines are drawn in the logarithmic mode in Figure 4. We have also compared the CPU times for solving this integral equation using the presented method ( $q = 2$ ) and the thin plate splines ( $k = 2$ ) for different numbers of  $N$  in Figure 5. It is seen that the CPU times of the proposed method are much lower than the thin plate splines which it confirms that the new approach is very fast in comparison to thin plate splines.

**Table 6.** Some numerical results for Example 5.3 with Gaussian weight functions

$N$	$h$	$\ e_N\ _2$		$\ e_N\ _\infty$		Ratio	Ratio
		$q = 1$	$q = 2$	$q = 1$	$q = 2$		
11	0.3111	$9.17 \times 10^{-5}$	$1.23 \times 10^{-6}$	$1.12 \times 10^{-4}$	—	$2.86 \times 10^{-6}$	—
21	0.2180	$4.52 \times 10^{-5}$	$9.08 \times 10^{-7}$	$6.21 \times 10^{-5}$	1.65	$1.26 \times 10^{-6}$	2.30
39	0.1601	$2.22 \times 10^{-5}$	$2.82 \times 10^{-7}$	$3.47 \times 10^{-5}$	1.88	$5.14 \times 10^{-7}$	2.91
58	0.1313	$1.08 \times 10^{-5}$	$1.19 \times 10^{-7}$	$2.36 \times 10^{-5}$	1.94	$2.87 \times 10^{-7}$	2.93
88	0.1066	$8.51 \times 10^{-6}$	$8.11 \times 10^{-8}$	$1.57 \times 10^{-5}$	1.95	$1.29 \times 10^{-7}$	3.83
105	0.0975	$5.14 \times 10^{-6}$	$3.78 \times 10^{-8}$	$1.25 \times 10^{-5}$	1.98	$9.14 \times 10^{-8}$	2.53

**Table 7.** Some numerical results for Example 5.3 with spline weight functions

$N$	$h$	$\ e_N\ _2$		$\ e_N\ _\infty$		Ratio	Ratio
		$q = 1$	$q = 2$	$q = 1$	$q = 2$		
11	0.3111	$4.89 \times 10^{-5}$	$8.92 \times 10^{-7}$	$8.35 \times 10^{-5}$	—	$1.41 \times 10^{-6}$	—
21	0.2180	$2.70 \times 10^{-5}$	$2.91 \times 10^{-7}$	$4.61 \times 10^{-5}$	1.67	$5.87 \times 10^{-7}$	2.46
39	0.1601	$1.21 \times 10^{-5}$	$1.21 \times 10^{-7}$	$2.57 \times 10^{-5}$	1.89	$2.38 \times 10^{-7}$	2.92
58	0.1313	$9.57 \times 10^{-6}$	$9.11 \times 10^{-8}$	$1.75 \times 10^{-5}$	1.93	$1.35 \times 10^{-7}$	2.85
88	0.1066	$7.89 \times 10^{-6}$	$3.82 \times 10^{-8}$	$1.16 \times 10^{-5}$	1.97	$6.21 \times 10^{-8}$	3.72
105	0.0975	$4.79 \times 10^{-6}$	$2.51 \times 10^{-8}$	$8.52 \times 10^{-6}$	1.94	$4.25 \times 10^{-8}$	2.63

**Example 5.3.** Consider the following Fredholm-Hammerstein integral equation:

$$u(x, t) - \int_D \frac{\ln(x^2 + s^2 + 1)}{t^2 + y^2 + e} \sqrt{u(y, s) + y + \pi} ds dy = f(x, t), \quad (x, t) \in D,$$

where the function  $f(x, t)$  has been so chosen that the exact solution is

$$u_{ex}(x, t) = \ln \left( 10 + \frac{xt + t}{x + t^2 + 1} \right),$$

and  $D$  is the tear domain drawn in Figure 6. Here we separate the domain  $D$  as  $D = D_1 \cup D_2$ , where

$$D_1 = \left\{ (x, t) \in \mathbb{R}^2 : 0 < x < 1, 0.5 < t < 0.5 + 0.25\sqrt{3x(3x-3)^2} \right\},$$

$$D_2 = \left\{ (x, t) \in \mathbb{R}^2 : 0 < x < 1, 0.5 - 0.25\sqrt{3x(3x-3)^2} < t < 0.5 \right\}.$$

The distribution of the nodes, selected randomly on the domain  $D$ , is depicted in Figure 7. The numerical results in terms of  $\|e_N\|_2$  and  $\|e_N\|_\infty$  at different numbers of  $N$  and the rate of convergence for the linear and quadratic basis functions utilizing the Gaussian and spline weight functions are presented in Tables 6 and 7, respectively. The obtained errors for different numbers of  $N$  are drawn in the logarithmic mode in Figure 8. Theorem 4.2 concludes that the results gradually converge to the exact values along with the increase of the nodes .i.e., for the linear basis  $\|u_{ex} - \hat{u}_N\| \approx \mathcal{O}(h^2)$  and for the quadratic basis  $\|u_{ex} - \hat{u}_N\| \approx \mathcal{O}(h^3)$ . Note that for the quadratic basis, for large  $N$ , the error near the boundary increases which consequently effects on the global error [45].

**Example 5.4.** As final example, we solve the following two-dimensional Fredholm integral equation:

$$u(x, t) - \int_D \frac{1+t+y}{e^{ts} \cosh(x+y)} \sin\left(\frac{u(y, s)}{\sqrt{y+s+6}}\right) ds dy = g(x, t), \quad (x, t) \in D,$$

where the function  $g(x, t)$  has been so chosen that the exact solution is

$$u_{ex}(x, t) = \frac{x^2 + 1}{\sqrt{x + t + 10}},$$

and  $D$  is the fish-like domain drawn in Figure 9. Here we can separate the domain  $D$  as  $D = D_1 \cup D_2$ , where

$$\begin{aligned} D_1 &= \{(x, t) \in \mathbb{R}^2 : 0 \leq x \leq 1, 0.5 \leq t \leq 0.5 + \sqrt{0.25 - (x - 0.5)^2}\}, \\ D_2 &= \{(x, t) \in \mathbb{R}^2 : 0.3 \leq x \leq 0.7, 0 \leq t \leq 0.5\}. \end{aligned}$$

The distribution of the nodes, selected randomly on the domain  $D$ , is depicted in Figure 10. The numerical results in terms of  $\|e_N\|_2$  and  $\|e_N\|_\infty$  at different numbers of  $N$  and the rate of convergence for the linear and quadratic basis functions utilizing the Gaussian and spline weight functions are presented in Tables 8 and 9, respectively. To compare the presented method, we also solve the integral equation (5.4) utilizing the thin plate splines and the numerical results are given in Table 10. The obtained errors for different numbers of  $N$  using the presented method and the thin plate splines are drawn in the logarithmic mode in Figure 11. We have also compared the CPU times for solving this integral equation using the presented method ( $q = 2$ ) and the thin plate splines ( $k = 2$ ) for different numbers of  $N$  in Figure 12. These results show the presented method in the current paper, in comparison with the method based on the thin plate splines for solving integral equations, uses much less computer memory and times. Moreover, the convergence rates of the new method are higher than the convergence rates of the thin plate splines.

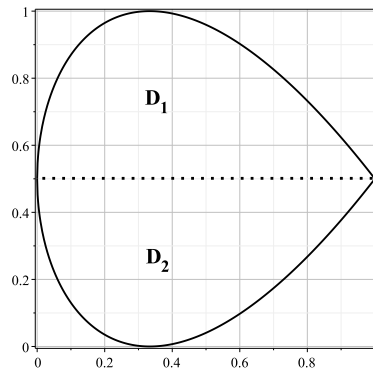


Figure 6. The consideration domain  $D$  for Example 5.3

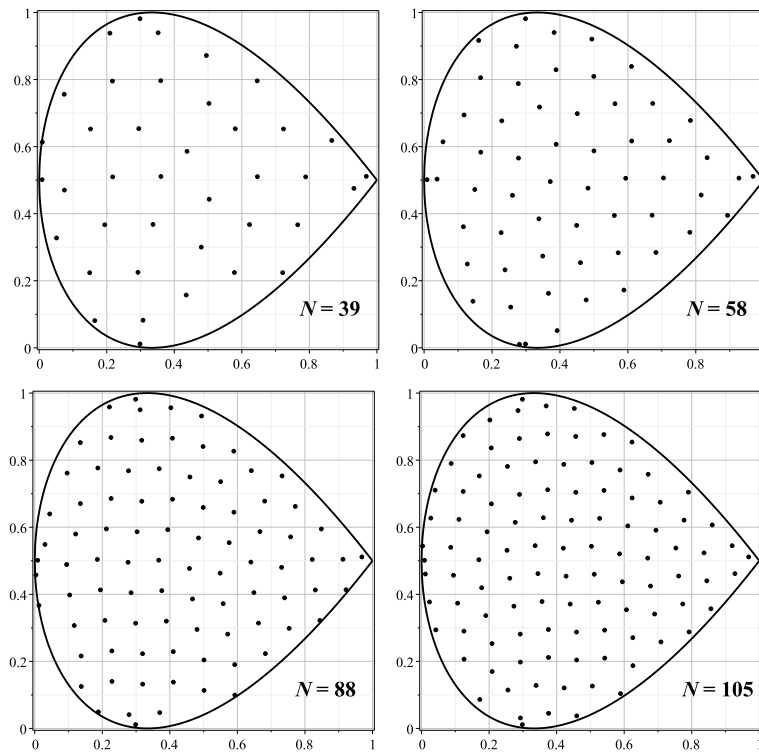


Figure 7. Node distribution for Example 5.3

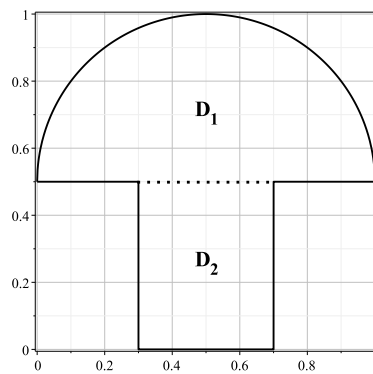


Figure 9. The consideration domain  $D$  for Example 5.4





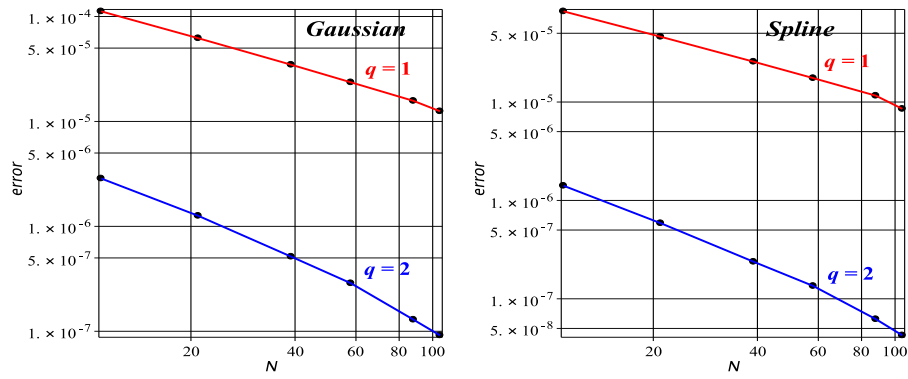


Figure 8. Absolute error distributions of Example 5.3

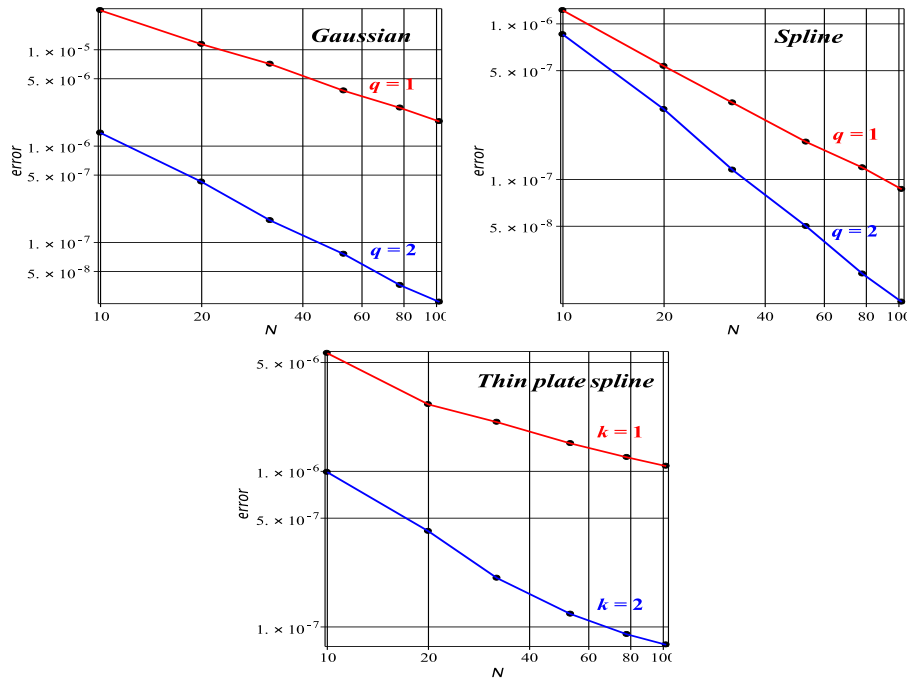


Figure 11. Absolute error distributions of Example 5.4

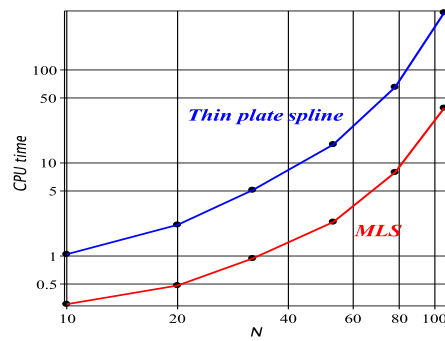


Figure 12. CPU times for Example 5.4

**Table 8.** Some numerical results for Example 5.4 with Gaussian weight functions

$N$	$h$	$\ e_N\ _2$		$\ e_N\ _\infty$		Ratio	Ratio
		$q = 1$	$q = 2$	$q = 1$	$q = 2$		
10	0.3360	$1.13 \times 10^{-5}$	$8.76 \times 10^{-7}$	$2.56 \times 10^{-5}$	—	$1.37 \times 10^{-6}$	—
20	0.1997	$7.42 \times 10^{-6}$	$2.11 \times 10^{-7}$	$1.14 \times 10^{-5}$	1.87	$4.25 \times 10^{-7}$	2.24
32	0.1428	$3.71 \times 10^{-6}$	$9.39 \times 10^{-8}$	$6.06 \times 10^{-6}$	1.95	$1.61 \times 10^{-7}$	2.89
53	0.1111	$1.66 \times 10^{-6}$	$4.51 \times 10^{-8}$	$3.71 \times 10^{-6}$	1.98	$7.56 \times 10^{-8}$	3.01
78	0.0909	$1.07 \times 10^{-6}$	$2.32 \times 10^{-8}$	$2.49 \times 10^{-6}$	1.88	$3.59 \times 10^{-8}$	3.71
102	0.0769	$7.36 \times 10^{-7}$	$1.21 \times 10^{-8}$	$1.80 \times 10^{-6}$	1.94	$2.41 \times 10^{-8}$	2.38

**Table 9.** Some numerical results for Example 5.4 with spline weight functions

$N$	$h$	$\ e_N\ _2$		$\ e_N\ _\infty$		Ratio	Ratio
		$q = 1$	$q = 2$	$q = 1$	$q = 2$		
10	0.3360	$9.17 \times 10^{-7}$	$5.22 \times 10^{-7}$	$1.22 \times 10^{-6}$	—	$8.54 \times 10^{-7}$	—
20	0.1997	$3.21 \times 10^{-7}$	$1.19 \times 10^{-7}$	$5.34 \times 10^{-7}$	1.58	$2.82 \times 10^{-7}$	2.13
32	0.1428	$1.23 \times 10^{-7}$	$7.21 \times 10^{-8}$	$2.81 \times 10^{-7}$	1.91	$1.05 \times 10^{-7}$	2.94
53	0.1111	$9.82 \times 10^{-8}$	$2.37 \times 10^{-8}$	$1.74 \times 10^{-7}$	1.90	$4.99 \times 10^{-8}$	2.96
78	0.0909	$8.32 \times 10^{-8}$	$1.12 \times 10^{-8}$	$1.19 \times 10^{-7}$	1.89	$2.47 \times 10^{-8}$	3.50
102	0.0769	$5.94 \times 10^{-8}$	$8.15 \times 10^{-9}$	$8.64 \times 10^{-8}$	1.91	$1.63 \times 10^{-8}$	2.49

**Table 10.** Some numerical results for Example 5.4 with thin plate splines

$N$	$h$	$\ e_N\ _2$		$\ e_N\ _\infty$		Ratio	Ratio
		$q = 1$	$q = 2$	$q = 1$	$q = 2$		
10	0.3360	$4.27 \times 10^{-6}$	$6.32 \times 10^{-7}$	$5.74 \times 10^{-6}$	—	$9.87 \times 10^{-7}$	—
20	0.1997	$1.83 \times 10^{-6}$	$3.24 \times 10^{-7}$	$2.49 \times 10^{-6}$	1.93	$4.12 \times 10^{-7}$	2.52
32	0.1428	$1.59 \times 10^{-6}$	$1.19 \times 10^{-7}$	$2.07 \times 10^{-6}$	1.48	$2.06 \times 10^{-7}$	2.95
53	0.1111	$9.37 \times 10^{-7}$	$7.48 \times 10^{-8}$	$1.51 \times 10^{-6}$	1.25	$1.21 \times 10^{-7}$	2.10
78	0.0909	$8.15 \times 10^{-7}$	$5.56 \times 10^{-8}$	$1.23 \times 10^{-6}$	1.06	$8.96 \times 10^{-8}$	1.55
102	0.0769	$6.84 \times 10^{-7}$	$4.21 \times 10^{-8}$	$1.08 \times 10^{-6}$	0.96	$7.68 \times 10^{-8}$	1.14

## 6. Conclusion

The main intention of the current paper has been to describe a scheme for the numerical solution of one- and two-dimensional Fredholm-Hammerstein integral equations of the second kind. These types of integral equations have been used as a mathematical model in various branches of applied science and engineering. The method is based on the discrete Galerkin method with the shape functions of the MLS approximation constructed on scattered points as a basis. The integrals appeared in this method have been approximated by a composite Gauss-Legendre integration rule. The proposed method does not require any domain element, so it is meshless and independent of the geometry of the domain. The numerical results for different examples have been reported to show the efficiency of the new method for solving various types of Hammerstein integral equations. All numerical results have confirmed the theoretical error estimates.

**Acknowledgements.** The authors are very grateful to both anonymous reviewers for their valuable comments and suggestions which have improved the paper.

## References

- [1] M. A. Abdou, A. A. Badr and M. B. Soliman, *On a method for solving a two-dimensional nonlinear integral equation of the second kind*, J. Comput. Appl. Math., 2011, 235(12), 3589–3598.
- [2] H. Adibi and P. Assari, *On the numerical solution of weakly singular Fredholm integral equations of the second kind using Legendre wavelets*, J. Vib. Control., 2011, 17(5), 689–698.
- [3] A. Alipanah and S. Esmaeili, *Numerical solution of the two-dimensional Fredholm integral equations using Gaussian radial basis function*, J. Comput. Appl. Math., 2011, 235(18), 5342–5347.
- [4] M. G. Armentano, *Error estimates in Sobolev spaces for moving least square approximations*, SIAM J. Numer. Anal., 2002, 39(1), 38–51.
- [5] M. G. Armentano and R. G. Duron, *Error estimates for moving least square approximations*, Appl. Numer. Math., 2001, 37(3), 397–416.
- [6] P. Assari, H. Adibi and M. Dehghan, *A meshless method for solving nonlinear two-dimensional integral equations of the second kind on non-rectangular domains using radial basis functions with error analysis.*, J. Comput. Appl. Math., 2013, 239(1), 72–92.
- [7] P. Assari, H. Adibi and M. Dehghan, *A numerical method for solving linear integral equations of the second kind on the non-rectangular domains based on the meshless method*, Appl. Math. Model., 2013, 37(22), 9269–9294.
- [8] P. Assari, H. Adibi and M. Dehghan, *A meshless discrete Galerkin (MDG) method for the numerical solution of integral equations with logarithmic kernels*, J. Comput. Appl. Math., 2014, 267, 160–181.
- [9] P. Assari, H. Adibi and M. Dehghan, *A meshless method based on the moving least squares (MLS) approximation for the numerical solution of two-dimensional nonlinear integral equations of the second kind on non-rectangular domains*, Numer. Algor., 2014, 67(2), 423–455.
- [10] P. Assari, H. Adibi and M. Dehghan, *The numerical solution of weakly singular integral equations based on the meshless product integration (MPI) method with error analysis*, Appl. Numer. Math., 2014, 81, 76–93.
- [11] P. Assari and M. Dehghan, *A meshless discrete Galerkin method based on the free shape parameter radial basis functions for solving Hammerstein integral equations*, Numer. Math. Theor. Meth. Appl., 2018, 11, 541–569.
- [12] P. Assari and M. Dehghan, *The numerical solution of two-dimensional logarithmic integral equations on normal domains using radial basis functions with polynomial precision*, Eng. Comput., 2017. DOI: 10.1007/s00366-017-0502-5.
- [13] K. E. Atkinson, *The numerical evaluation of fixed points for completely continuous operators*, SIAM J. Numer. Anal., 1973, 10, 799–807.
- [14] K. E. Atkinson, *The Numerical Solution of Integral Equations of the Second Kind*, Cambridge University Press, Cambridge, 1997.
- [15] K. E. Atkinson and A. Bogomolny, *The discrete Galerkin method for integral equations*, Math. Comp., 1987, 48, 595–616.

- 
- [16] K. E. Atkinson and J. Flores, *The discrete collocation method for nonlinear integral equations*, IMA J. Numer. Anal., 1993, 13(2), 195–213.
- [17] E. Babolian, S. Bazm and P. Lima, *Numerical solution of nonlinear two-dimensional integral equations using rationalized Haar functions*, Commun. Nonlinear. Sci. Numer. Simulat., 2011, 16(3), 1164–1175.
- [18] S. Bazm and E. Babolian, *Numerical solution of nonlinear two-dimensional Fredholm integral equations of the second kind using gauss product quadrature rules*, Commun. Nonlinear. Sci. Numer. Simulat., 2012, 17(3), 1215–1223.
- [19] M. D. Buhmann, *Radial Basis Functions: Theory and Implementations*, Cambridge University Press, Cambridge, 2003.
- [20] V. Carutasu, *Numerical solution of two-dimensional nonlinear Fredholm integral equations of the second kind by spline functions*, General. Math., 2001, 9, 31–48.
- [21] W. Chen and W. Lin, *Galerkin trigonometric wavelet methods for the natural boundary integral equations*, Appl. Math. Comput., 2001, 121(1), 75–92.
- [22] P. Dasa, G. Nelakantia and G. Longb, *Discrete Legendre spectral projection methods for Fredholm-Hammerstein integral equations*, J. Comput. Appl. Math., 2015, 278, 293–305.
- [23] M. Dehghan and R. Salehi, *The numerical solution of the non-linear integro-differential equations based on the meshless method*, J. Comput. Appl. Math., 2012, 236(9), 2367–2377.
- [24] W. Fang, Y. Wang and Y. Xu, *An implementation of fast wavelet Galerkin methods for integral equations of the second kind*, J. Sci. Comput., 2004, 20(2), 277–302.
- [25] R. Farengo, Y.C. Lee and P.N. Guzdar, *An electromagnetic integral equation: Application to microtearing modes*, Phys. Fluids, 1983, 26(12), 3515–3523.
- [26] G. E. Fasshauer, *Meshfree methods*, In: Handbook of Theoretical and Computational Nanotechnology, American Scientific Publishers, 2005.
- [27] A. Golbabai and S. Seifollahi, *Numerical solution of the second kind integral equations using radial basis function networks*, Appl. Math. Comput., 2006, 174(2), 877–883.
- [28] I. G. Graham, *Collocation methods for two dimensional weakly singular integral equations*, J. Austral. Math. Soc. (Series B), 1993, 22, 456–473.
- [29] L. Grammonta, P. B. Vasconcelos and M. Ahuesa, *A modified iterated projection method adapted to a nonlinear integral equation*, Appl. Math. Comput., 2016, 276, 432–441.
- [30] H. Guoqiang and W. Jiong, *Extrapolation of Nystrom solution for two dimensional nonlinear Fredholm integral equations*, J. Comput. Appl. Math., 2001, 134(1–2), 259–268.
- [31] H. Guoqiang and W. Jiong, *Richardson extrapolation of iterated discrete Galerkin solution for two-dimensional Fredholm integral equations*, J. Comput. Appl. Math., 2002, 139, 49–63.
- [32] H. Guoqiang, W. Jiong, K. Hayami and X. Yuesheng, *Correction method and extrapolation method for singular two-point boundary value problems*, J. Comput. Appl. Math., 2000, 126(1–2), 145–157.

- [33] R. Hanson and J. Phillips, *Numerical solution of two-dimensional integral equations using linear elements source*, SIAM J. Numer. Anal., 1978, 15, 113–121.
- [34] H. Kaneko and Y. Xu, *Gauss-type quadratures for weakly singular integrals and their application to Fredholm integral equations of the second kind*, Math. Comp., 1994, 62(206), 739–753.
- [35] H. Kaneko and Y. Xu, *Superconvergence of the iterated Galerkin methods for Hammerstein equations*, SIAM J. Numer. Anal., 1996, 33(3), 1048–1064.
- [36] B. Kress, *Linear Integral Equations*, Springer-Verlag, Berlin, 1989.
- [37] S. Kumar, *A discrete collocation-type method for Hammerstein equations*, SIAM J. Numer. Anal., 1998, 25(2), 328–341.
- [38] S. Kumar and I. H. Sloan, *A new collocation type method for Hammerstein integral equations*, Math. Comput., 1987, 48(178), 585–593.
- [39] P. Lancaster and K. Salkauskas, *Surfaces generated by moving least squares methods*, Math. Comput., 1981, 37(155), 141–158.
- [40] X. Li, *Meshless Galerkin algorithms for boundary integral equations with moving least square approximations*, Appl. Numer. Math., 2011, 61(12), 1237–1256.
- [41] X. Li and J. Zhu, *A Galerkin boundary node method and its convergence analysis*, J. Comput. Appl. Math., 2009, 230(1), 314–328.
- [42] X. Li and Q. Wang, *Analysis of the inherent instability of the interpolating moving least squares method when using improper polynomial bases*, Eng. Anal. Bound. Elem., 2016, 73, 21–34.
- [43] X. Li, H. Chen and Y. Wang, *Error analysis in Sobolev spaces for the improved moving least-square approximation and the improved element-free Galerkin method*, Appl. Math. Comput., 2015, 262, 56–78.
- [44] A. V. Manzhirov, *On a method of solving two-dimensional integral equations of axisymmetric contact problems for bodies with complex rheology*, J. Appl. Math. Mech., 1985, 49(6), 777–782.
- [45] D. Mirzaei and M. Dehghan, *A meshless based method for solution of integral equations*, Appl. Numer. Math., 2010, 60(3), 245–262.
- [46] Y. Ordokhani, *Solution of Fredholm-Hammerstein integral equations with walsh-hybrid functions*, Int. Math. Forum., 2009, 4, 969–976.
- [47] K. Parand and J. A. Rad, *Numerical solution of nonlinear Volterra-Fredholm-Hammerstein integral equations via collocation method based on radial basis functions*, Appl. Math. Comput., 2012, 218(9), 5292–5309.
- [48] A. Pedas and G. Vainikko, *Product integration for weakly singular integral equations in  $m$  dimensional space*, In: B. Bertram, C. Constanda, A. Struthers (Ed.), *Integral Methods in Science and Engineering*, 280–285, Chapman and Hall/CRC, 2000.
- [49] A. Quarteroni, R. Sacco and F. Saleri, *Numerical Analysis for Electromagnetic Integral Equations*, Artech House, Boston, 2008.
- [50] A. Tari, M. Y. Rahimi, S. Shahmorad and F. Talati, *Solving a class of two-dimensional linear and nonlinear Volterra integral equations by the differential transform method*, J. Comput. Appl. Math., 2009, 228(1), 70–76.

- 
- [51] A. M. Wazwaz, *Linear and Nonlinear Integral equations: Methods and Applications*, Higher Education Press and Springer Verlag, Heidelberg, 2011.
- [52] H. Wendland, *Scattered Data Approximation*, Cambridge University Press, New York, 2005.